

Degradation of entanglement between two accelerated parties: Bell states under the Unruh effect

Benedikt Richter^{1,2} and Yasser Omar^{1,2,3}

¹*Physics of Information Group, Instituto de Telecomunicações, Portugal*

²*Instituto Superior Técnico, Universidade de Lisboa, Portugal and*

³*CEMAPRE, ISEG, Universidade de Lisboa, Portugal*

(Dated: March 12, 2019)

We study the entanglement of families of Unruh modes in the Bell states $|\Phi^\pm\rangle = 1/\sqrt{2}(|00\rangle \pm |11\rangle)$ and $|\Psi^\pm\rangle = 1/\sqrt{2}(|01\rangle \pm |10\rangle)$ shared by two accelerated observers, and find fundamental differences in the robustness of entanglement against acceleration for these states. States Ψ^\pm are entangled for all finite accelerations, whereas, due to the Unruh effect, states Φ^\pm lose their entanglement for finite accelerations. This is true for Bell states of two bosonic modes, as well as for Bell states of a bosonic and a fermionic mode. But also for Bell states of fermionic modes there are differences in the degradation of entanglement. We reveal the origin of these distinct characteristics of entanglement degradation and discuss the role that is played by particle statistics. Our studies suggest that the behavior of entanglement in accelerated frames strongly depends on the occupation patterns of the constituent states, whose superposition constitutes the entangled state, where especially states Φ^\pm and Ψ^\pm exhibit distinct characteristics regarding entanglement degradation. Finally, we point out possible implications of hovering over a black hole for these states.

PACS numbers: 03.67.Mn, 03.65.-w, 03.65.Ud, 04.62.+v

I. INTRODUCTION

Entanglement and quantum correlations in general play an important role in different areas of physics, as, for example, in quantum information [1] and in black holes [2, 3]. Furthermore, it is known that the quantum correlations of an entangled state shared by accelerated observers are not invariant with respect to acceleration but are altered by the Unruh effect [4]. Interestingly, the non-invariance of quantum correlations in this relativistic regime can be employed to carry out quantum information tasks [5–9]. Although accelerated motion can, in some special cases, create entanglement between Unruh modes [10], generally entanglement is degraded due to the Unruh effect.

In the past, the degradation of entanglement in bipartite states composed of Unruh modes shared by an inertial observer and an uniformly accelerated one was studied in detail [11–23]. For fermionic fields, entanglement approaches a finite value in the infinite acceleration limit [11], while for bosons it vanishes asymptotically [4]. One way to study the entanglement between two accelerated observers is to analyse an entangled state shared by three parties, where two parties are in accelerated motion, and subsequently trace out the inertial observer [24–26]. A more natural way to study entanglement in this framework is to restrict to bosonic entanglement in accelerated two-mode squeezed states and to use tools from continuous variable quantum mechanics [27, 28]. There it was found that, for these squeezed states, entanglement vanishes for finite accelerations, in contrast to the entanglement of states shared by an accelerated observer and an inertial one.

As realized more recently in [29–31], there are some caveats in the interpretation of states of Unruh modes.

But still, the use of Unruh modes, that allows for closed analytical solutions, provides a valuable framework to understand the mechanisms that lead to a decrease of quantum correlations in entangled states, when described by accelerated observers. The goal of this work is to provide further insight into the degradation of entanglement that occurs when entangled states are observed by accelerated parties. Therefore, in this work, we study families of states composed of Unruh modes that are maximally entangled from the inertial perspective and investigate the residual entanglement when these states are seen by uniformly accelerated observers.

We start by studying the entanglement between two accelerated observers sharing the fermionic Bell states $|\Phi^\pm\rangle = 1/\sqrt{2}(|0_\omega 0_\Omega\rangle \pm |1_\omega 1_\Omega\rangle)$ and $|\Psi^\pm\rangle = 1/\sqrt{2}(|0_\omega 1_\Omega\rangle \pm |1_\omega 0_\Omega\rangle)$. We find that entanglement is non-vanishing for all accelerations, and that the degradation of quantum correlations depends on the specific state shared by the parties. The reason for the survival of entanglement for fermions is rooted in the statistics obeyed by fermions, while the state-dependence of entanglement degradation seems to be originated in the occupation pattern of the state that is shared between the two observers. By occupation pattern we mean the pattern of both constituent states (in the following just called constituents), for example, $|00\rangle$, $|01\rangle$, $|10\rangle$ and $|11\rangle$, whose superposition defines the entangled state. That is, the set of excitations created by the Unruh effect depends on the state one starts with.

Furthermore, we study maximally entangled bosonic states shared by two accelerated observers and, in contrast to [27, 28, 32], we consider two bosonic modes of frequency ω and Ω , respectively, in the Bell states Φ^\pm and Ψ^\pm . We find that the Unruh effect degrades entanglement in these two states very differently. While, as

in [27, 28, 32], bosonic modes in state Φ^\pm lose all their entanglement for finite accelerations, the entanglement of these modes in state Ψ^\pm is non-vanishing for all finite accelerations. We find that this crucial difference in the degradation of entanglement is due to the differing occupation patterns of the constituents of the two Bell states, and is manifest in the appearance of a “cut off function” in the expression of the negativity.

Then, we extend our studies to accelerated states of a bosonic mode maximally entangled with a fermionic one. Thereby we find states whose negativity factorizes. But, due to the bosonic mode involved in these states, there is no entanglement surviving in the infinite acceleration limit. Then, moving on to Bell states Φ^\pm and Ψ^\pm , we obtain qualitatively the same behavior as for the purely bosonic Bell states. Thus, we find evidence for the importance of the occupation patterns of the constituents. The particular occupation patterns of its constituents can protect a state’s entanglement against the effects of acceleration, i.e. the Unruh effect. Using an effective state picture we are able to explain the differences in the behavior.

In the past, the different behavior of the entanglement of accelerated fermions and bosons led to some discussions [13, 18, 22]. Here we address this issue and discuss the role played by particle statistics by combining the results of the fermion-fermion, boson-boson and the boson-fermion cases. We conclude that there are essentially two factors determining the fading of entanglement, where one is purely from particle statistics and one strongly depends on the occupation patterns of the constituents of the state that is considered. Finally, we discuss some effects hovering over a black hole at a fixed distance from the horizon has on the entanglement of the states that are studied in this work.

The outline is the following. In Section II we give a short introduction to quantum fields in Rindler space. In Sections III, IV and V we study the entanglement of fermion-fermion, boson-boson and boson-fermion Bell states in accelerated motion, respectively. Then, in Section VI, we discuss the role of particle statistics for entanglement degradation and give two factors that determine the characteristics of said degradation. In VII we outline possible implications of our findings for Bell states in the vicinity of a black hole and, finally, in VIII, we give the conclusions of this work.

For the sake of brevity, throughout this work, we will call the occupation patterns of the constituents of a state just the structure of a state.

II. QUANTUM FIELDS IN RINDLER SPACE

We give a brief introduction to quantum field theory in Rindler space. The main purpose is to introduce the framework we are using in this work. More details can be found, for example, in [14, 33, 34]. We will work in units where $c = \hbar = k_B = 1$. Minkowski coordinates

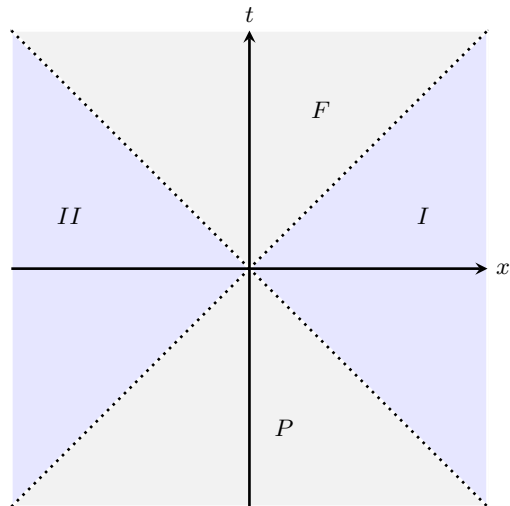


FIG. 1: Rindler space: Regions *I* and *II* are causally disconnected due to the presence of horizons at $x = t$ and $x = -t$.

(t, x) and Rindler coordinates (ξ, η) are related by the following transformations

$$t = \xi \sinh(\eta), \quad (1a)$$

$$x = \xi \cosh(\eta), \quad (1b)$$

where the range of ξ and η is given by $-\infty < \xi, \eta < \infty$. Notice that ξ is positive in the right wedge (region *I*) and ξ is negative in the left wedge (region *II*). Then we obtain the following metric

$$ds^2 = \xi^2 d\eta^2 - d\xi^2. \quad (2)$$

Considering a world line with $\xi(\tau) = \frac{1}{a}$, where τ is the proper time along this trajectory and $|a|$ is the proper acceleration, we find $\eta(\tau) = a\tau$. Thus, in Minkowski coordinates the world line reads $t(\tau) = \frac{1}{a} \sinh(a\tau)$, $x(\tau) = \frac{1}{a} \cosh(a\tau)$. As shown in Figure 1, the two regions *I* and *II* of Rindler space are causally disconnected due to the presence of horizons at $x = t$ and $x = -t$. A timelike Killing vector in region *I* is given by ∂_η ($-\partial_\eta$ in *II*).

A. Bosons

We consider the quantization of a massless scalar field ϕ (see [33, 34] for details). We quantize fields with respect to the Killing vectors ∂_η and $-\partial_\eta$ independently in the two regions. The Klein-Gordon equation $\square\phi = 0$ in Rindler coordinates has solutions which depend on η as [34]

$$u_\omega^\pm \propto e^{\pm i\tilde{\omega}\eta}, \quad \pm \partial_\eta u_\omega^\pm = i\tilde{\omega} u_\omega^\pm, \quad (3)$$

where $\tilde{\omega}$ is a positive parameter and the sign \pm depends on the Rindler wedge. These modes are positive frequency modes with respect to the respective timelike

Killing vectors. We denote by $u_{\tilde{\omega}}^{I,II}$, i.e. $u_{\tilde{\omega}}^I \propto e^{-i\tilde{\omega}\eta}$ and $u_{\tilde{\omega}}^{II} \propto e^{+i\tilde{\omega}\eta}$, the solutions in region I and II , respectively. We can expand ϕ in this basis and obtain

$$\phi = \int_0^\infty d\tilde{\omega} \left(a_{\tilde{\omega}}^I u_{\tilde{\omega}}^I + a_{\tilde{\omega}}^{I\dagger} u_{\tilde{\omega}}^{I*} + a_{\tilde{\omega}}^{II} u_{\tilde{\omega}}^{II} + a_{\tilde{\omega}}^{II\dagger} u_{\tilde{\omega}}^{II*} \right), \quad (4)$$

where the $a_{\tilde{\omega}}^{I/II}$ and $a_{\tilde{\omega}}^{I/II\dagger}$ are the usual commuting annihilation and creation operators in regions I and II . The dependence on the proper time $\tau = \frac{\eta}{a}$ is given by $u_{\tilde{\omega}}^I \propto e^{-ia\tilde{\omega}\tau}$. Therefore, the energy ω seen by the accelerated observer is given by $\omega = a\tilde{\omega}$. Remember that in Minkowski space ϕ can be expanded as

$$\phi = \int_0^\infty d\omega_M \left(a_{\omega_M}^M u_{\omega_M}^M + a_{\omega_M}^{M\dagger} u_{\omega_M}^{M*} \right), \quad (5)$$

where $a_{\omega_M}^M$ and $a_{\omega_M}^{M\dagger}$ are the commuting Minkowski annihilation and creation operators. These two expansions lead to different Fock spaces. Consider the Minkowski (M) vacuum $|0\rangle_M$ and the Rindler (R) vacuum $|0\rangle_R = |0\rangle_I \otimes |0\rangle_{II}$ that are defined as

$$a_{\omega_M}^M |0\rangle_M = 0, \quad (6a)$$

$$a_{\tilde{\omega}}^I |0\rangle_R = a_{\tilde{\omega}}^{II} |0\rangle_R = 0 \quad (6b)$$

and in general $a_{\tilde{\omega}}^{I,II} |0\rangle_M \neq 0$. Next, we want to introduce the so called Unruh basis that we will use in the following. The Rindler creation and annihilation operators $a_{\tilde{\omega}}^{I,II}$ are related to the corresponding Unruh (U) ones $a_{\tilde{\omega}}^{U,1,2}$ by a Bogoliubov transformation as follows [33]

$$a_{\tilde{\omega}}^I = \frac{1}{\sqrt{2 \sinh(\pi\tilde{\omega})}} \left(e^{\frac{\pi\tilde{\omega}}{2}} a_{\tilde{\omega}}^{U,2} + e^{-\frac{\pi\tilde{\omega}}{2}} a_{\tilde{\omega}}^{U,1\dagger} \right), \quad (7a)$$

$$a_{\tilde{\omega}}^{II} = \frac{1}{\sqrt{2 \sinh(\pi\tilde{\omega})}} \left(e^{\frac{\pi\tilde{\omega}}{2}} a_{\tilde{\omega}}^{U,1} + e^{-\frac{\pi\tilde{\omega}}{2}} a_{\tilde{\omega}}^{U,2\dagger} \right). \quad (7b)$$

These share the positive frequency analyticity properties of the $u_{\omega_M}^M$ and therefore have the same vacuum state $a_{\tilde{\omega}}^{U,1,2} |0\rangle_M = 0$, i.e. $|0\rangle_U = |0\rangle_M$ [35].

In this work we study accelerated observers confined to Rindler wedge I and work in the Unruh basis. To obtain the appropriate description of what an accelerated observer is experiencing, we use Bogoliubov transformations (7) to go from the Unruh basis to the Rindler basis. For an Unruh mode $\tilde{\omega}$, the vacuum and one particle states are given by

$$|0_{\tilde{\omega}}\rangle_U = \sum_n \frac{\tanh^n(r)}{\cosh(r)} |n_{\tilde{\omega}}\rangle_I |n_{\tilde{\omega}}\rangle_{II}, \quad (8a)$$

$$|1_{\tilde{\omega}}\rangle_U = \sum_n \frac{\tanh^n(r)}{\cosh^2(r)} \sqrt{n+1} |n+1_{\tilde{\omega}}\rangle_I |n_{\tilde{\omega}}\rangle_{II} \quad (8b)$$

for a massless uncharged scalar field, where the acceleration parameter r is set by $\tilde{\omega}$ and they are related by $r = \operatorname{arctanh}(e^{-\pi\tilde{\omega}})$. Further, $|n\rangle_I$ and $|n\rangle_{II}$ are the n -particle states in regions I and II , respectively. Note

that in (8b) we denote the one-particle state $a_{\tilde{\omega}}^{U,2\dagger} |0_{\tilde{\omega}}\rangle_U$ by $|1_{\tilde{\omega}}\rangle_U$. That is, the excitation is localized in I . Similarly, for a massless charged scalar field the vacuum and one-particle states are given by [18]

$$|0_{\tilde{\omega}}\rangle_U = \sum_{n,m} \frac{\tanh^{n+m}(r)}{\cosh^2(r)} |nm\rangle_I |nm\rangle_{II}, \quad (9a)$$

$$|1_{\tilde{\omega}}\rangle_U^+ = \sum_{n,m} \frac{\tanh^{n+m}(r)}{\cosh^3(r)} \sqrt{n+1} |(n+1)m\rangle_I |nm\rangle_{II}, \quad (9b)$$

$$|1_{\tilde{\omega}}\rangle_U^- = \sum_{n,m} \frac{\tanh^{n+m}(r)}{\cosh^3(r)} \sqrt{m+1} |n(m+1)\rangle_I |nm\rangle_{II}, \quad (9c)$$

where $|nm\rangle_R$ denotes the state of m/n particles/ anti-particles of energy $\tilde{\omega}$ in region $R = I, II$.

B. Fermions

We will model the fermionic field by a massless Grassmannian valued scalar field ψ . Then the quantization of ψ can be carried out analogously to the bosonic case. To obtain the appropriate description of what an accelerated observer is experiencing, we use the Bogoliubov transformations [14]

$$a_{\tilde{\omega}}^I = \frac{1}{\sqrt{2 \cosh(\pi\tilde{\omega})}} \left(e^{\frac{\pi\tilde{\omega}}{2}} a_{\tilde{\omega}}^{U,2} + e^{-\frac{\pi\tilde{\omega}}{2}} a_{\tilde{\omega}}^{U,1\dagger} \right), \quad (10a)$$

$$a_{\tilde{\omega}}^{II} = \frac{1}{\sqrt{2 \cosh(\pi\tilde{\omega})}} \left(e^{\frac{\pi\tilde{\omega}}{2}} a_{\tilde{\omega}}^{U,1} + e^{-\frac{\pi\tilde{\omega}}{2}} a_{\tilde{\omega}}^{U,2\dagger} \right) \quad (10b)$$

to go from the Unruh basis to the Rindler basis. We choose the notation $|ijkl\rangle_{\tilde{\omega}} = |i_{\tilde{\omega}}\rangle_I^+ \otimes |j_{\tilde{\omega}}\rangle_{II}^- \otimes |k_{\tilde{\omega}}\rangle_I^- \otimes |l_{\tilde{\omega}}\rangle_{II}^+$, where $+/-$ denote particles and anti-particles, respectively, and obtain for an Unruh mode $\tilde{\omega}$

$$\begin{aligned} |0_{\tilde{\omega}}^F\rangle_U &= \cos^2(r_f) |0000\rangle_{\tilde{\omega}} - \cos(r_f) \sin(r_f) |0011\rangle_{\tilde{\omega}} \\ &\quad + \cos(r_f) \sin(r_f) |1100\rangle_{\tilde{\omega}} - \sin^2(r_f) |1111\rangle_{\tilde{\omega}}, \end{aligned} \quad (11a)$$

$$|1_{\tilde{\omega}}^F\rangle_U^+ = \cos(r_f) |1000\rangle_{\tilde{\omega}} - \sin(r_f) |1011\rangle_{\tilde{\omega}}, \quad (11b)$$

$$|1_{\tilde{\omega}}^F\rangle_U^- = \cos(r_f) |0010\rangle_{\tilde{\omega}} + \sin(r_f) |1110\rangle_{\tilde{\omega}}, \quad (11c)$$

where the acceleration parameter r_f is given by $r_f = \operatorname{arctan}(e^{-\pi\tilde{\omega}})$.

C. Unruh effect

An accelerated observer does not necessarily agree with an inertial observer on the number of particles in a given state. Consider, for example, the fermionic Minkowski vacuum state $|0\rangle_M = |0\rangle_U \equiv |0\rangle$. Then the

vacuum expectation value of the (Rindler) number operator $\langle 0|a_{\tilde{\omega}}^{I/II\dagger}a_{\tilde{\omega}}^{I/II}|0\rangle$ can be calculated using (10), leading to

$$\langle 0|a_{\tilde{\omega}}^{I/II\dagger}a_{\tilde{\omega}}^{I/II}|0\rangle = 1 + e^{\frac{2\pi\omega}{a}}. \quad (12)$$

Thus, we see that an accelerated observer perceives the Minkowski vacuum as a thermal state of temperature T_U (Unruh temperature) [35]

$$T_U = \frac{a}{2\pi}. \quad (13)$$

Further, we introduce the fermionic and the bosonic partition functions Z_F^ω and Z_B^ω that are given by

$$Z_B^\omega = \frac{1}{1 - e^{-\frac{2\pi\omega}{a}}} = \frac{1}{1 - e^{-\frac{\omega}{T_U}}}, \quad (14)$$

$$Z_F^\omega = 1 + e^{-\frac{2\pi\omega}{a}} = 1 + e^{-\frac{\omega}{T_U}}. \quad (15)$$

There are some subtleties when working with the global Unruh modes (8), (9), (11), as pointed out in [29–31]. Therefore, one point that we want to emphasize is the implicit dependence on the acceleration a in (7) and (10) through the relation $\tilde{\omega} = \frac{\omega}{a}$. As a consequence, after fixing the frequency ω , each of the Unruh modes (8), (9), (11) forms a family of modes that is labeled by a . That is, by varying the acceleration parameter r/r_f (or equivalently a) one also varies the particular Unruh mode under consideration. In order to pick a particular state, ω and a have to be fixed. Intuitively, one can say that the acceleration a is already encoded in the Unruh modes. We will revisit these issues when we discuss the entanglement of fermions in Section III. In the following, for the sake of simplicity, we omit the tilde in $\tilde{\omega}$ whenever it is clear from the context whether we are talking about ω or $\tilde{\omega}$.

In this brief introduction to quantum fields in Rindler space we have set up the tools and notation we are using in the following. In the next section we study the degradation of entanglement in fermionic Bell states due to acceleration.

III. ENTANGLEMENT AND ENTROPY OF UNIFORMLY ACCELERATED FERMION STATES

Due to the anti-commutativity of fermionic creation/annihilation operators (Pauli Exclusion Principle) there is only a finite number of maximally entangled states of two modes of a fermionic field. Considering particle states, there are just two possible maximally entangled states. These are the two Bell states of two fermionic modes (FF)

$$|\Psi_{FF}^\pm\rangle = \frac{1}{\sqrt{2}} (|1_\omega^F\rangle_U |0_\Omega^F\rangle_U \pm |0_\omega^F\rangle_U |1_\Omega^F\rangle_U), \quad (16a)$$

$$|\Phi_{FF}^\pm\rangle = \frac{1}{\sqrt{2}} (|0_\omega^F\rangle_U |0_\Omega^F\rangle_U \pm |1_\omega^F\rangle_U |1_\Omega^F\rangle_U). \quad (16b)$$

The subscript U emphasizes that we are working in the Unruh basis.

A. Negativity

We consider two families of entangled fermionic Unruh modes ω and Ω undergoing constant accelerations a_ω and a_Ω , respectively. The acceleration parameters of the modes are denoted by r_f^ω and r_f^Ω . Therefore, starting from the families of states $\{\psi_i\} = \{\Psi_{FF}^\pm, \Phi_{FF}^\pm\}$ written in the Unruh basis, we use (11) to obtain the density matrices $\rho_{I,II}^{(i)}$

$$\rho_{I,II}^{(i)} = |\psi_i\rangle\langle\psi_i|. \quad (17)$$

To describe the system as it is seen by an observer confined to region I , we have to trace out modes that have their support in the inaccessible region. Then the reduced density matrix ρ_i is given by

$$\rho_i = \text{Tr}_{II} \left(\rho_{I,II}^{(i)} \right). \quad (18)$$

As a measure of entanglement we use the negativity N , which is an entanglement monotone [36]. The negativity for a composite system (we denote the subsystems by A and B) described by a density matrix $\rho = \rho_{AB}$ is given by the sum of the absolute values of the negative eigenvalues of the partially transposed density matrix ρ_{AB}^{pT}

$$N = \frac{1}{2} \sum_j (|\lambda_j| - \lambda_j), \quad (19)$$

where the λ_j 's are the eigenvalues of ρ_{AB}^{pT} . It is known that a bipartite state is not separable if its negativity is non-zero [37]. Furthermore, the vanishing of the negativity provides a necessary and sufficient condition for the separability of mixed states of two qubits [38]. Fermions, in general, cannot be treated as qubits. But, when charge superselection is respected, two fermionic modes can be represented as two qubits [39]. A further property of the negativity is that a state with vanishing negativity contains no distillable (free) entanglement, although, in this case, there can be non-distillable (bound) entanglement present [40]. In this work, we will ignore the possibility of bound entanglement and refer to free entanglement as entanglement.

To obtain the negativities N_i of states ψ_i , we have to calculate the partially transposed reduced density matrices ρ_i^{pT} . We find that these matrices are block diagonal. More details of the calculations can be found in Appendix A. The final results for the negativities N_i read

$$N_{\Psi_{FF}^\pm} = \frac{1}{2} \left(\sqrt{\frac{1}{Z_F^\omega} \frac{1}{Z_F^\Omega} + \left(\frac{n_F^\omega + n_F^\Omega}{2} \right)^2} - \frac{n_F^\omega + n_F^\Omega}{2} \right), \quad (20)$$

$$N_{\Phi_{FF}^\pm} = \frac{1}{2} \frac{1}{Z_F^\omega} \frac{1}{Z_F^\Omega}, \quad (21)$$

where $T_{\omega/\Omega}$ are the Unruh temperatures (13) corresponding to the respective accelerations a_ω and a_Ω , $Z_F^{\omega/\Omega}$ is the partition function (15) and ω , Ω are the energies of the modes. Further, we introduced the occupation numbers $n_F^\omega = (1 + e^{\omega/T_\omega})^{-1}$ and $n_F^\Omega = (1 + e^{\Omega/T_\Omega})^{-1}$.

Having obtained the analytic expressions for the negativities of the families of maximally entangled fermion states (16), we want to comment on the physical interpretation of these states. As discussed in Section II, we are not describing a fixed state ψ_i , but rather describe a two-parameter family of states ψ_i labeled by a_ω and a_Ω . Therefore, the negativities (20) and (21) give the entanglement of the states ψ_i (maximally entangled from the inertial perspective), when the two modes ω and Ω are seen by accelerated observers undergoing the accelerations a_ω and a_Ω , respectively. Equivalently, we can think of states ψ_i as families labeled by ω and Ω , when we are fixing a_ω and a_Ω . It should be noted that for a given set $(\omega, \Omega, a_\omega, a_\Omega)$ the only difference between these states is the difference in their occupation pattern, in the sense of $|00\rangle + |11\rangle$ vs. $|10\rangle + |01\rangle$. In the following, we discuss the effects of acceleration on these families of states and, for sake of brevity, refer to them just as states.

Considering state Φ_{FF}^\pm , it is interesting to note that the negativity (21) factorizes as follows

$$N_{\Phi_{FF}^\pm}(r_f^\omega, r_f^\Omega) = 2N_f(r_f^\omega)N_f(r_f^\Omega), \quad (22)$$

where we denoted $N_{\Phi_{FF}^\pm}(r_f^\omega, r_f^\Omega = 0)$ by $N_f(r_f^\omega)$. Note that $N_f(r_f^\omega)$ is the negativity in case of only one mode being seen by an accelerated observer (acceleration parameter r_f^ω). The negativity $N_f(r_f^\omega) = \frac{1}{2} \cos^2(r_f^\omega)$ was obtained, for example, in [13]. This product structure is absent for state Ψ_{FF}^\pm , where the negativity is given by (20). Thus, the degradation of entanglement in the case of a fermionic field shows no universal behavior. Indeed different classes of states, Ψ_{FF}^\pm and Φ_{FF}^\pm , are not equally robust against acceleration, see Figure 2.

There is a fundamental difference between states Φ_{FF}^\pm and Ψ_{FF}^\pm . While each state ψ_i is a superposition of two states (constituents) of the form $|k_\omega^F\rangle_U |l_\Omega^F\rangle_U$ ($k, l \in \{0, 1^+\}$), only for state Ψ_{FF}^\pm both such states lead to a contribution to a (the same) diagonal element of the reduced density matrix that is relevant for entanglement. More precisely, for non-vanishing acceleration, $|1_\omega^F\rangle_U |0_\Omega^F\rangle_U$ as well as $|0_\omega^F\rangle_U |1_\Omega^F\rangle_U$ contribute to the matrix element $|1_\omega^F\rangle_I |1_\Omega^F\rangle_I \langle 1_\omega^F| \langle 1_\Omega^F|$ of the reduced density matrix. This is well reflected in the expression for the negativity, given by (20). The contribution of $|1_\omega^F\rangle_U |0_\Omega^F\rangle_U$ is quantified by n_F^ω and the one of $|0_\omega^F\rangle_U |1_\Omega^F\rangle_U$ by n_F^Ω . Due to the symmetry, (20) depends only the average occupation number $\bar{n}_F = 1/2(n_F^\omega + n_F^\Omega)$. This behavior distinguishes Ψ_{FF}^\pm from Φ_{FF}^\pm .

As in the setting of one mode seen by an accelerated observer and one mode seen by an inertial observer [13, 14, 20], in the limit of infinite acceleration the negativity does not vanish, but it approaches a finite limit. The

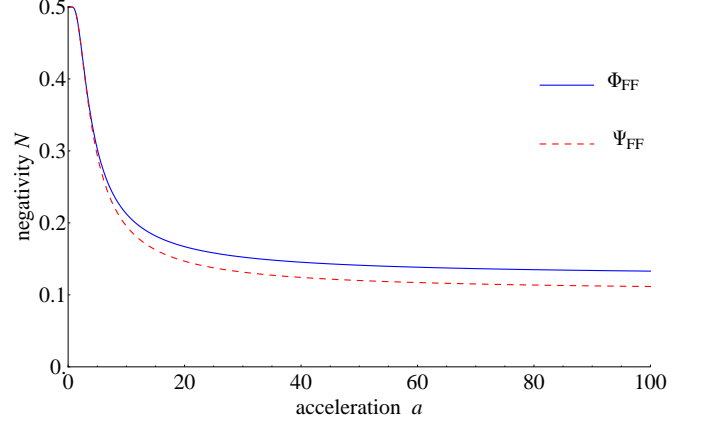


FIG. 2: Negativities for maximally entangled fermion states $\{\psi_i\}$ versus acceleration $a = a_\omega = a_\Omega$ for $\omega = 1$, $\Omega = 1$. For each fixed acceleration a , the entanglement degradation for state Φ_{FF}^\pm (blue, continuous) is stronger than for state Ψ_{FF}^\pm (red, dashed). The finite asymptotic values for state Φ_{FF}^\pm and Ψ_{FF}^\pm are $1/8$ and $1/4(\sqrt{2} - 1)$, respectively.

surviving entanglement is calculated to be

$$\lim_{r_f^\omega, r_f^\Omega \rightarrow \infty} N_{\Phi_{FF}^\pm} = \frac{1}{8}, \quad (23a)$$

$$\lim_{r_f^\omega, r_f^\Omega \rightarrow \infty} N_{\Psi_{FF}^\pm} = \frac{1}{4} (\sqrt{2} - 1). \quad (23b)$$

The fact that there is entanglement surviving in this limit is specific for initially pure maximally entangled states and contrasts with the case of starting from a tripartite state, where one observer is inertial and two observers are accelerated. In that case, after tracing out the inertial observer, the bipartite entanglement between the modes observed by accelerated observers vanishes in this limit [24]. Numerical studies of fermionic mixed state entanglement also showed that entanglement is extinguished for most states in the infinite acceleration limit [41].

Our results reduce to the known results for one accelerated observer if one takes the limit $r_f^\Omega \rightarrow 0$ and we obtain the universal behavior reported in [13]

$$\lim_{r_f^\Omega \rightarrow 0} N_i \equiv N_f = \frac{1}{2} \cos^2(r_f^\omega) \quad (24)$$

and thus

$$\lim_{r_f^\omega \rightarrow \infty} N_f = \frac{1}{4}. \quad (25)$$

Interestingly, the behavior of the negativity under acceleration does not depend on whether there is entanglement created in some sectors or not. We define a sector of a state ψ_i as follows: A sector of state ψ_i consists of all the elements of the reduced density matrix ρ_i that

contribute to one block of the block diagonal partially transposed reduced density matrix ρ_i^{pT} . For example, Φ_{FF}^\pm has four sectors, as can be seen from the partially transposed reduced density matrix $\rho_{\Phi_{FF}^\pm}^{pT}$ (see (A1) in Appendix A). When the acceleration is increasing from zero, entanglement decreases in the sector where it is initiated and, depending on the particular structure of the state, entanglement is created in previously non-entangled sectors. More details can be found in Appendix A 2.

The consequences of the fact that states (11) depend on the acceleration $a_{\omega/\Omega}$ only via the ratios ω/a_ω and Ω/a_Ω are manifest in (20) and (21). One observes that high frequency modes are less effected by acceleration than low frequency modes are. This is due to the larger wavelength of low energy modes. The larger the wavelength, and therefore the spatial extension, compared to the inverse Unruh temperature, the more the system gets “stretched” by the acceleration. Thus the effects of acceleration are stronger in this case and the rate of entanglement degradation is higher.

To summarize, there is no universality in the degradation of entanglement for maximally entangled fermion states if both modes are seen by accelerated observers. That is a feature that was absent in previous studies of one accelerated observer. Furthermore, it can be seen from (23) that there is less surviving entanglement in the case of two accelerated observers. For state Φ_{FF}^\pm the negativity approaches exactly one half of the limiting value of N_f , while the entanglement in Ψ_{FF}^\pm is degraded even further. Entanglement is non-vanishing in initially maximally entangled fermion states due to the finiteness of the fermionic partition function Z_F , that is due to the relative small number of states allowed by the Pauli Exclusion Principle and by the number of different excitations (particles and anti-particles). Acceleration “just causes rotations” in the initial states.

Finally, we again want to emphasize that the negativities shown in Figure 2 do not represent the negativity of a fixed entangled pair of fermions seen by accelerated observers of dynamically varying acceleration a . Instead, for each set $(\omega, \Omega, a_\omega, a_\Omega)$, the negativity, as it is observed by two accelerated observers (of acceleration a_ω and a_Ω , respectively), of a different state that is maximally entangled when seen by inertial observers, is shown. Therefore, the conclusion that the degradation of entanglement depends on the class of the state ψ_i holds irrespective of the problems related to working with Unruh modes.

After this detailed study of the negativity of states (16), we now move on to analyse the entropy and the mutual information of these states. This provides further insight into the effects acceleration has on the correlations in fermion states.

B. Entropy and mutual information

In the following, we analyse entropy and mutual information of the fermion states. Since we are considering accelerated observers and therefore trace out region II to obtain the reduced density matrices ρ_i , the resulting state is not pure any more. Thus, the entropy of ρ_i increases due to entanglement with modes in region II . Among the different measures of entropy, the most widely used is the von Neumann entropy S , given by

$$S(\rho_i) = -\text{Tr}_I(\rho_i \log(\rho_i)). \quad (26)$$

Usually the von Neumann entropy S is hard to calculate and so sometimes the Rényi-2 entropy S_2 is used instead. In our setting, the von Neumann entropy can be calculated analytically. Since the corresponding expressions are quite long and not very enlightening, we give the plots of S as a function of the acceleration in Figure 3. In the limit of infinite acceleration the von Neumann entropies approach the asymptotic values $S^\infty(\rho_i)$, that are given in the following

$$S^\infty(\rho_{\Phi_{FF}^\pm}) = \frac{\log(32)}{4} - \frac{3 + 2\sqrt{2}}{8} \log\left(\frac{3 + 2\sqrt{2}}{32}\right) + \frac{2\sqrt{2} - 3}{8} \log\left(\frac{3 - 2\sqrt{2}}{32}\right), \quad (27a)$$

$$S^\infty(\rho_{\Psi_{FF}^\pm}) = \log(8). \quad (27b)$$

The Rényi-2 entropy S_2 is given by the formula

$$S_2(\rho_i) = -\log(\text{Tr}_I \rho_i^2). \quad (28)$$

For more details, including the analytical expressions of S_2 , see Appendix A 3.

Furthermore, we calculate the mutual information I between modes ω and Ω as a measure of quantum and classical correlations as

$$I_i = S(\text{Tr}_\omega(\rho_i)) + S(\text{Tr}_\Omega(\rho_i)) - S(\rho_i), \quad (29)$$

where $\text{Tr}_{\omega/\Omega}$ denotes the trace over mode ω/Ω . The resulting mutual information of states $\{\psi_i\}$ (in bits) is shown in Figure 3. In the limit of infinite acceleration the surviving correlations are given by I_i^∞ :

$$I_{\Phi_{FF}^\pm}^\infty = \frac{1}{8 \log(2)} (-\log\left(\frac{531441}{256}\right) + (3 + 2\sqrt{2}) \log(3 + 2\sqrt{2}) + (3 - 2\sqrt{2}) \log(3 - 2\sqrt{2})), \quad (30a)$$

$$I_{\Psi_{FF}^\pm}^\infty = \frac{1}{\log(2)} \log\left(\frac{8}{3\sqrt{3}}\right). \quad (30b)$$

As it can be seen from Figure 3, the entanglement entropies vanish for zero acceleration, as the mode is localized in region I . So there is no entanglement between

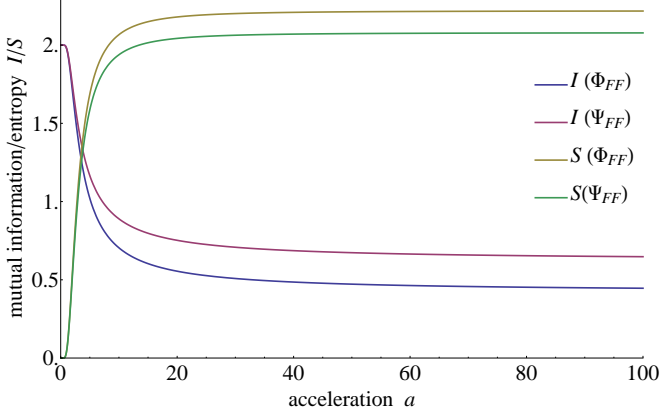


FIG. 3: Mutual information, measured in bits, and von Neumann entropy for maximally entangled fermion states $\{\psi_i\}$ plotted versus acceleration $a = a_\omega = a_\Omega$ for frequencies $\omega = \Omega = 1$. The mutual information of states Φ_{FF}^\pm and Ψ_{FF}^\pm , as well as the entropies of these states approach different asymptotic values.

modes in region I and modes in region II . As the acceleration increases, an acceleration horizon forms and the entanglement entropy increases due to tracing out modes with support in the region behind the horizon. We see that the entanglement between modes in the accessible region and modes in the inaccessible region does not increase equally for all states, but depends on the particular ψ_i . The mutual information of states Φ_{FF}^\pm and Ψ_{FF}^\pm decreases with increasing acceleration and, in the infinite acceleration limit, approaches distinct values ($I_{\Phi_{FF}^\pm}^\infty \approx 0.4$, $I_{\Psi_{FF}^\pm}^\infty \approx 0.6$). Since $I_i^\infty < 1$ for all states, we conclude that also classical correlations become degraded

with increasing acceleration.

In this Section we studied the degradation of quantum and classical correlations in fermion states that is caused by uniform acceleration. In the following Section we study the entanglement in bosonic Bell states.

IV. ENTANGLEMENT OF UNIFORMLY ACCELERATED BOSON-BOSON STATES

We continue by investigating the entanglement of Bell states of Unruh modes ω and Ω of a massless uncharged scalar field

$$|\Psi_{BB}^\pm\rangle = \frac{1}{\sqrt{2}} (|0_\omega\rangle_U |1_\Omega\rangle_U \pm |1_\omega\rangle_U |0_\Omega\rangle_U), \quad (31a)$$

$$|\Phi_{BB}^\pm\rangle = \frac{1}{\sqrt{2}} (|0_\omega\rangle_U |0_\Omega\rangle_U \pm |1_\omega\rangle_U |1_\Omega\rangle_U), \quad (31b)$$

where ω, Ω are the frequencies and 0, 1 the occupation numbers of the Unruh-modes. We consider the two modes ω and Ω undergoing constant accelerations a_ω and a_Ω , respectively. The acceleration parameters of the modes are denoted by r^ω and r^Ω . We write states (31) in the Rindler basis to obtain the infinite dimensional density matrices $\rho_{I,II}^{(i=\Psi^\pm, \Phi^\pm)}$. Then, to describe the system as it is seen by an observer confined to region I , we have to trace out modes that have their support in region II .

As in Section III, to obtain the negativities N_i of states (31), we determine the partially transposed reduced density matrices ρ_i^{pT} that are block diagonal and calculate the negative eigenvalues. More details can be found in Appendix B. The negativities of Bell states (31) are given by the following expressions

$$N_{\Psi_{BB}^\pm} = \frac{1}{2} \frac{1}{(Z_B^\omega)^2} \frac{1}{(Z_B^\Omega)^2} \left(\sqrt{Z_B^\omega Z_B^\Omega + \frac{1}{4} (n_B^\omega + n_B^\Omega)^2} - \frac{1}{2} (n_B^\omega + n_B^\Omega) \right) + \sum_{n=1}^{\infty} N_{\Psi_{BB}^\pm}^{(n)}, \quad (32)$$

$$N_{\Phi_{BB}^\pm} = \frac{1}{2} \frac{1}{(Z_B^\omega)^2} \frac{1}{(Z_B^\Omega)^2} \gamma_{\Phi_{BB}^\pm} (n_B^\omega, n_B^\Omega) + \sum_{n=1}^{\infty} N_{\Phi_{BB}^\pm}^{(n,0)} + \sum_{m=1}^{\infty} N_{\Phi_{BB}^\pm}^{(0,m)}, \quad (33)$$

where $n_B^\omega = (e^{\frac{\omega}{T_\omega}} - 1)^{-1}$ ($n_B^\Omega = (e^{\frac{\Omega}{T_\Omega}} - 1)^{-1}$) is the Bose-Einstein distribution with the Unruh temperatures $T_\omega/T_\Omega = \frac{a_\omega/a_\Omega}{2\pi}$, $Z_B^{\omega/\Omega}$ is the bosonic partition function (14) and $\gamma_{\Phi_{BB}^\pm}$ is given by

$$\gamma_{\Phi_{BB}^\pm} = 1 - n_B^\omega n_B^\Omega. \quad (34)$$

$N_{\Psi_{BB}^\pm}^{(n)}$, $N_{\Phi_{BB}^\pm}^{(n,0)}$ and $N_{\Phi_{BB}^\pm}^{(0,m)}$ give small corrections compared to the leading term and can be found in Appendix B. The degradation of entanglement shows fundamen-

tally different characteristics for the two Bell states Ψ_{BB}^\pm and Φ_{BB}^\pm , see Figure 4. While for Ψ_{BB}^\pm entanglement vanishes asymptotically, Φ_{BB}^\pm loses all its entanglement for finite acceleration.

In case of Ψ_{BB}^\pm , for $r^\omega = r^\Omega$, only one of the blocks on the diagonal of the partially transposed reduced density matrix admits negative eigenvalues. There is no entanglement generated in any sector and only the sector, where entanglement is initialized, contributes to the negativity $N_{\Psi_{BB}^\pm}$. From now on, we refer to a sector as all

elements of the reduced density matrix that contribute to one block of the block diagonal partially transposed reduced density matrix. For $r^\omega \neq r^\Omega$ there is entanglement created in all sectors.

Note that the negativity vanishes asymptotically. The reason, why Ψ_{BB}^\pm does not become non-distillable (and therefore does not become separable) for any finite acceleration is that the occupation of state $|00\rangle$ is always zero, i.e. the Unruh effect does not drive the occupation of this state. This is due to the fact that the constituents of Ψ_{BB}^\pm both contain one excitation and, thus, state $|00\rangle$ is not accessible. In consequence the matrix element $|00\rangle\langle 00|$ in $\rho_{\Psi_{BB}^\pm}$ is always zero and entanglement vanishes only asymptotically for infinite acceleration, as in this regime all occupation is shifted towards highly excited states.

As we show in Appendix B, the negativity of Φ_{BB}^\pm is of the form $N_{\Phi_{BB}^\pm} = \sum_{n,m=0}^{\infty} N_{\Phi_{BB}^\pm}^{(n,m)}$ and it can be seen that each of the $N_{\Phi_{BB}^\pm}^{(n,m)}$ is bounded from above by $N_{\Phi_{BB}^\pm}^{(0)} \equiv N_{\Phi_{BB}^\pm}^{(0,0)}$. The (partial) negativity $N_{\Phi_{BB}^\pm}^{(0)}$ can be read off from (33)

$$N_{\Phi_{BB}^\pm}^{(0)} = \frac{1}{2} \frac{1}{(Z_B^\omega)^2} \frac{1}{(Z_B^\Omega)^2} \gamma_{\Phi_{BB}^\pm}(n_B^\omega, n_B^\Omega), \quad (35)$$

where $\gamma_{\Phi_{BB}^\pm}$ is some kind of “cut off function”. As all $N_{\Phi_{BB}^\pm}^{(n,m)}$ are bounded from above by $N_{\Phi_{BB}^\pm}^{(0)}$, it follows that $N_{\Phi_{BB}^\pm}$ vanishes for the same parameters as $N_{\Phi_{BB}^\pm}^{(0)}$ does. These parameters are characterized by $n_B^\omega n_B^\Omega = 1$, i.e. as soon as this fraction of the population is excited to the first state above the vacuum, state Φ_{BB}^\pm loses its entanglement.

This can be understood in an intuitive picture considering an effective state represented by an effective density matrix $\rho_{eff}^{\Phi_{BB}^\pm}(k)$ of the k th sector. As we saw, the block diagonal nature of the partially transposed reduced density matrix $\rho_{\Phi_{BB}^\pm}^{pT}$ leads to a negativity of the form $N_{\Phi_{BB}^\pm} = N_{\Phi_{BB}^\pm}^{(0)} + \sum_{n=1}^{\infty} N_{\Phi_{BB}^\pm}^{(n,0)} + \sum_{m=1}^{\infty} N_{\Phi_{BB}^\pm}^{(0,m)}$. So we introduce $\rho_{eff}^{\Phi_{BB}^\pm}(k)$ such that the negative eigenvalue of $\left(\rho_{eff}^{\Phi_{BB}^\pm}\right)^{pT}(k)$ provides $N_{\Phi_{BB}^\pm}^{(k,0)}$. Although there is not a strict symmetry between n and m in (33), the effective description captures the essential features of the behavior of entanglement, as the vanishing of $N_{\Phi_{BB}^\pm}^{(k,0)}$ implies that $N_{\Phi_{BB}^\pm}^{(0,k)}$ is vanishing as well. Imagine that only one observer is accelerated ($a_\omega \neq 0$) while the other one is inertial ($a_\Omega = 0$), then we can write an effective state $\rho_{eff}^\omega(k)$ as

$$\begin{aligned} \rho_{eff}^\omega(k) = & \alpha_k(a_\omega) |0k\rangle\langle 1(k+1)| + \\ & + \beta_k(a_\omega) |0(k+1)\rangle\langle 0(k+1)| + \\ & + \delta_k(a_\omega) |1k\rangle\langle 1k| + \\ & + \gamma_k(a_\omega) |1(k+1)\rangle\langle 0k|, \end{aligned} \quad (36)$$

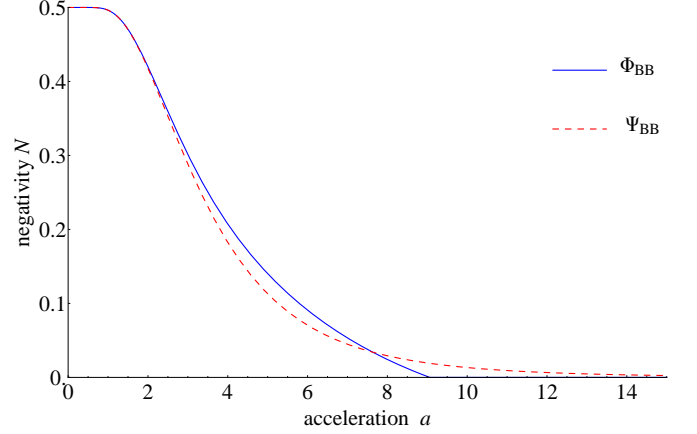


FIG. 4: Negativities for the maximally entangled boson states Φ_{BB}^\pm and Ψ_{BB}^\pm , where both observers are accelerated, plotted against acceleration $a = a_\omega = a_\Omega$ for $\omega = 1$, $\Omega = 1$. The negativity of state Φ_{BB}^\pm (blue, continuous) vanishes for finite accelerations, while the negativity of Ψ_{BB}^\pm (red, dashed) vanishes asymptotically.

where $\delta_k(a_\omega) \equiv 0$ and we denoted $|n_\Omega\rangle_I \otimes |m_\omega\rangle_I$ by $|nm\rangle$. The coherences that are present in the initial state and are responsible for entanglement are quantified by $\alpha_0(a_\omega)$ and $\gamma_0(a_\omega)$. The coefficients $\beta_k(a_\omega)$ and $\delta_k(a_\omega)$ have the physical interpretation of quantifying the occupation of the states $|0(k+1)\rangle$ and $|1k\rangle$, respectively. Note that the Unruh effect drives the occupation of these states (in the present case only the occupation of $|0(k+1)\rangle$). Initially $\beta_k(a_\omega) = \delta_k(a_\omega) = 0$. Now it is easy to see that, for fixed k , (36) is always entangled for finite acceleration, but loses its entanglement for $a_\omega \rightarrow \infty$, as in this limit $\alpha_k, \beta_k, \gamma_k \rightarrow 0$ and thus $\alpha_k = \beta_k = \delta_k = \gamma_k = 0$. This explains why for one accelerated observer (like in [4]) entanglement vanishes in the infinite acceleration limit but not for finite accelerations.

Moving to the general case of $a_\omega \neq 0$, $a_\Omega \neq 0$, the effective density matrix of the k -excitation sector is of the form

$$\begin{aligned} \rho_{eff}^{\Phi_{BB}^\pm}(k) = & \alpha_k(a_\omega, a_\Omega) |0k\rangle\langle 1(k+1)| + \\ & + \beta_k(a_\omega, a_\Omega) |0(k+1)\rangle\langle 0(k+1)| + \\ & + \delta_k(a_\omega, a_\Omega) |1k\rangle\langle 1k| + \\ & + \gamma_k(a_\omega, a_\Omega) |1(k+1)\rangle\langle 0k| \end{aligned} \quad (37)$$

and the negativity vanishes for finite acceleration, i.e. $\alpha_k = \beta_k = \delta_k = \gamma_k \neq 0$ for $a_\omega, a_\Omega < \infty$. The equality between the strength of the coherences and the occupation of states $|0(k+1)\rangle$ and $|1k\rangle$, i.e. $\alpha_k = \beta_k = \delta_k = \gamma_k$, is achieved due to the special structure of the reduced density matrix $\rho_{\Phi_{BB}^\pm}$ (cf. (B2)).

Let us have a look at the $k = 0$ sector, where entanglement is initialized. For vanishing acceleration there are the coherences $|00\rangle\langle 11|$ and $|11\rangle\langle 00|$ that are non-vanishing, while the states $|10\rangle$ and $|01\rangle$ are not occu-

pied, i.e. $\beta_0 = \delta_0 = 0$; this state is maximally entangled. By increasing the acceleration the symmetry of the term $a_m^2 a_n^2 |nm\rangle\langle nm|$ in the reduced density matrix $\rho_{\Phi_{BB}^\pm}$ (cf. (B2)) leads to an equal occupation of $|10\rangle\langle 10|$ and $|01\rangle\langle 01|$. At the same time the coherences $|00\rangle\langle 11|$ and $|11\rangle\langle 00|$ are decreasing symmetrically. So for some finite acceleration $\alpha_0 = \beta_0 = \delta_0 = \gamma_0 \neq 0$ holds and entanglement vanishes.

But there is also entanglement creation in sectors of higher excitations $k > 0$ that are initially unoccupied in the sense of $\alpha_k = \beta_k = \delta_k = \gamma_k = 0$. Although entanglement is initially increasing in these sectors due to acceleration, it is vanishing for the same acceleration as in the $k = 0$ sector. This is due to the fact that besides $a_m^2 a_n^2 |nm\rangle\langle nm|$ also $\bar{a}_m^2 \bar{a}_n^2 |(n+1)(m+1)\rangle\langle (n+1)(m+1)|$ (cf. (B2)) drives the occupation of $|1k\rangle\langle 1k|$ and therefore compensates part of the loss of occupation of that state that is caused by the acceleration. This might be called “diagonal mixing” and is essential for achieving $\alpha_k \gamma_k = \beta_k \delta_k$ for finite acceleration. This condition is satisfied when $n_B^\omega n_B^\Omega = 1$ holds. The fact that both modes “smear out” due to the acceleration enables $\delta_k \neq 0$. This is the crucial point that enables the complete loss of entanglement for a finite acceleration.

Before moving on, we want to emphasize the dependence of the negativity on the energy of the modes. The condition for entanglement is given by

$$e^{-\frac{\omega}{T_\omega}} + e^{-\frac{\Omega}{T_\Omega}} \leq 1 \quad (38)$$

and we see that entanglement is more persistent for higher frequency modes. We introduced the Unruh temperature $T_{\omega/\Omega} = \frac{a_{\omega/\Omega}}{2\pi}$. Interestingly, in case of a two-mode squeezed state [28] the condition for entanglement is also given by (38). In the continuous variable case the vanishing of the negativity is a sufficient condition for separability [42], i.e. for bosonic two-mode squeezed states there is no bound entanglement once (38) is violated. In contrast, in the present case there might be some bound entanglement remaining in Φ_{BB}^\pm .

Further, it is interesting to note that we can write condition (38), for the same acceleration for both modes, i.e. $a_\omega = a_\Omega = a$, equivalently as

$$\omega \geq T \log(Z_B^\Omega) = -F_\Omega, \quad (39)$$

where $T = \frac{a}{2\pi}$ and $F_\Omega = -T \log(Z_B^\Omega)$ is the Helmholtz free energy. Note that the same condition with ω and Ω interchanged also holds. So at least formally the Helmholtz free energy of one mode bounds the energy (frequency) of the other one.

To summarize, by increasing the acceleration, i.e. by scanning through the families of states, entanglement decreases for all bosonic Bell states. But there is also entanglement created in sectors that have not been entangled initially. State Φ_{BB}^\pm loses all its entanglement for a finite value of the acceleration, whereas Ψ_{BB}^\pm is entangled for all finite accelerations. This is due to the appearance of

the function $\gamma_{\Phi_{BB}^\pm}$ that indicates the presence of a threshold, where the state becomes non-entangled. The reason for this behavior are the different occupation patterns of the constituents (structures) of the states we considered here. The negativities for the states are plotted in Figure 4. In contrast to the fermion case (cf. Section III) all states lose their entanglement in the infinite acceleration limit. This is due to the infinite tower of excitations for bosonic modes that leads to a partition function Z_B that grows unbounded. Since the negativities are proportional to Z_B^{-l} , where l is some positive integer, they approach zero for infinite accelerations. Intuitively speaking the acceleration leads to a temperature that shifts the occupation to higher energy states and therefore the occupation of the lowest lying states approaches zero. Our findings provide evidence that the structure of the states plays an important role, as this decides about the set of states that are accessible. The “noise” introduced by the Unruh effect is state dependent.

Next, after having addressed the bosonic case, we investigate the degradation of entanglement between a bosonic and a fermionic mode due to acceleration.

V. ENTANGLEMENT OF UNIFORMLY ACCELERATED BOSON-FERMION STATES

Using the same techniques as in Sections III and IV, we study the degradation of entanglement in boson-fermion states. We start by considering the non-Bell states

$$|X_1\rangle = \frac{1}{\sqrt{2}} (|0_\omega\rangle_U |1_\Omega^F\rangle_U^+ + |1_\omega\rangle_U |1_\Omega^F\rangle_U^-), \quad (40a)$$

$$|X_2\rangle = \frac{1}{\sqrt{2}} (|1_\omega\rangle_U^+ |1_\Omega^F\rangle_U^- + |1_\omega\rangle_U^- |1_\Omega^F\rangle_U^+), \quad (40b)$$

where F labels the fermionic mode, ω, Ω are the frequencies and 0, 1 the occupation numbers of the Unruh-modes. + and - refer to particles and antiparticles, respectively. The mode of frequency ω is bosonic while the mode of frequency Ω is fermionic. The respective acceleration parameters are given by $r = \text{arctanh}(e^{-\frac{\pi\omega}{a_\omega}})$ for the bosonic and $r_f = \text{arctan}(e^{\frac{\pi\Omega}{a_\Omega}})$ for the fermionic mode.

Again we use the negativity (19) as a measure of entanglement and obtain

$$N_{X_1} = 2N_f N_{b,1}, \quad (41)$$

$$N_{X_2} = 2N_f N_{b,2}, \quad (42)$$

where N_f is the (universal) negativity that was found for maximally entangled fermions $N_f = \frac{1}{2} \cos^2(r_f) = \frac{1}{2} (Z_F^\Omega)^{-1}$ [13] and $N_{b,1}, N_{b,2}$ are given by

$$N_{b,1} = \frac{1}{2} \frac{1}{(Z_B^\omega)^2} + \sum_{n=1}^{\infty} N_n, \quad (43)$$

$$N_{b,2} = \frac{1}{2} \frac{1}{Z_B^\omega}. \quad (44)$$

These are the negativities in the case that only the bosons are accelerated (Appendix B). Details of the calculations, as well as the expression for N_n , can be found in Appendix C.

Thus the degradation of entanglement in states X_1 and X_2 is quite similar to the behavior reported in [4]. Intuitively, what happens is the following. When accelerated the fermions get “rotated” and the bosons “smeared out”. Therefore, the fermions that are less affected by acceleration “mimic” the non-accelerated bosons. On the level of the partially transposed reduced density matrices we observe that the fermionic and the bosonic part factorize and thus the resulting negativity can be expressed in terms of negativities obtained from the cases of one accelerated observer.

But, as we will see, this is not a generic feature and it is absent in case of the boson-fermion Bell states Ψ_{BF}^\pm and Φ_{BF}^\pm that are given by

$$|\Psi_{BF}^\pm\rangle = \frac{1}{\sqrt{2}} (|1_\omega\rangle_U |0_\Omega^F\rangle_U \pm |0_\omega\rangle_U |1_\Omega^F\rangle_U^+), \quad (45a)$$

$$|\Phi_{BF}^\pm\rangle = \frac{1}{\sqrt{2}} (|0_\omega\rangle_U |0_\Omega^F\rangle_U \pm |1_\omega\rangle_U |1_\Omega^F\rangle_U^+). \quad (45b)$$

The negativities of states (45) are of the form $N = \sum_n N_n$ and again each of the N_n is bounded from above by N_0 . Remember that N_0 measures the negativity in the sector, where the entanglement is initialized. In the following we denote N_0 by $N_{\Psi_{BF}^\pm/\Phi_{BF}^\pm}^{(0)}$. The further N_n for $n \neq 0$ can be obtained analytically (Appendix C). But, already with the expression for $N_{\Psi_{BF}^\pm/\Phi_{BF}^\pm}^{(0)}$ in hand, we are able to characterize $N_{\Psi_{BF}^\pm/\Phi_{BF}^\pm}$. For states Ψ_{BF}^\pm and Φ_{BF}^\pm we obtain

$$N_{\Psi_{BF}^\pm} = N_{\Psi_{BF}^\pm}^{(0)} + \sum_{n=1}^{\infty} N_{\Psi_{BF}^\pm}^{(n)}, \quad (46)$$

$$N_{\Phi_{BF}^\pm} = N_{\Phi_{BF}^\pm}^{(0)} + \sum_{n=1}^{\infty} N_{\Phi_{BF}^\pm}^{(n)}, \quad (47)$$

where

$$N_{\Psi_{BF}^\pm}^{(0)} = \frac{1}{2} \frac{1}{Z_F^\Omega} \frac{1}{(Z_B^\omega)^2}, \quad (48)$$

$$N_{\Phi_{BF}^\pm}^{(0)} = \frac{1}{2} \frac{1}{Z_F^\Omega} \frac{1}{(Z_B^\omega)^2} \gamma_{\Phi_{BF}^\pm}(n_B^\omega, n_F^\Omega). \quad (49)$$

Further Z_B^ω , Z_F^Ω are the partition functions (14), (15), $n_B^\omega = (e^{\frac{\omega}{T_\omega}} - 1)^{-1}$ is the Bose-Einstein distribution, $n_F^\Omega = (e^{\frac{\Omega}{T_\Omega}} + 1)^{-1}$ is the Fermi-Dirac distribution and the T_ω/Ω are the Unruh temperatures introduced by the acceleration. The function $\gamma_{\Phi_{BF}^\pm}$ is given by

$$\gamma_{\Phi_{BF}^\pm} = \sqrt{\frac{n_B^\omega}{n_F^\Omega}} - n_B^\omega. \quad (50)$$

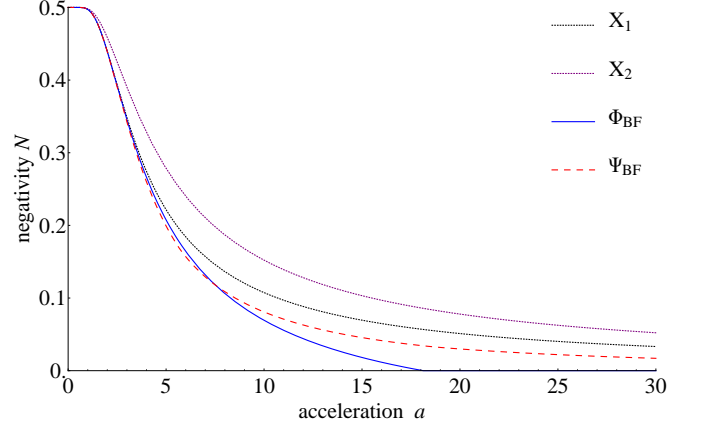


FIG. 5: Negativities for the maximally entangled boson-fermion states X_1 , X_2 , Φ_{BF}^\pm and Ψ_{BF}^\pm , where both observers are accelerated, plotted against acceleration $a = a_\omega = a_\Omega$ for $\omega = 1$, $\Omega = 1$. The degradation of entanglement occurs at different rates. The negativity of state Φ_{BF}^\pm (blue, continuous) vanishes for finite accelerations, while the negativities of X_1 (red, dashed), X_2 (purple, dashed) and Ψ_{BF}^\pm (black, continuous) vanish asymptotically.

Details of the calculations and the expressions for $N_{\Phi_{BF}^\pm}^{(n)}$ and $N_{\Psi_{BF}^\pm}^{(n)}$ can be found in Appendix C. The $N_{\Psi_{BF}^\pm/\Phi_{BF}^\pm}^{(0)}$ bound all the $N_{\Psi_{BF}^\pm/\Phi_{BF}^\pm}^{(n)}$ from above and therefore capture the essential behavior of entanglement degradation. So in the following we restrict our discussion to these quantities and refer to them as negativity.

In case of state Ψ_{BF}^\pm , the negativity is given by a product of the inverse partition functions for fermions and bosons. So the negativity vanishes in the infinite acceleration limit due to the unboundedness of the bosonic partition function. As for Ψ_{BB}^\pm in Section IV, the reason why $N_{\Psi_{BF}^\pm}^{(0)}$ is positive definite for finite accelerations is that there are no contributions to the density matrix of the form $|00\rangle\langle 00|$, since these cannot be created by the Unruh effect for states Ψ^\pm .

Moving to state Φ_{BF}^\pm , we realize that similarly to (35) the negativity of state Φ_{BF}^\pm vanishes for finite accelerations. Furthermore, as in (35), the threshold depends on the occupation numbers of the excited modes n_B^ω and n_F^Ω . When the product $n_B^\omega n_F^\Omega$ equals one, the negativity of state Φ_{BF}^\pm vanishes. So the threshold condition is of the same form as for Φ_{BB}^\pm , where it is given by $n_B^\omega n_F^\Omega = 1$. But, why does the negativity of Φ_{BF}^\pm vanish while states X_1 , X_2 and Ψ_{BF}^\pm are entangled for all finite accelerations? First, we note that if either r or r_f is vanishing, Φ_{BF}^\pm is entangled for all finite accelerations. To find the answer for the generic case, we use an effective state description,

as in Section IV, by

$$\rho_{eff}^{\pm}(k) = \rho_{eff,1}^{\pm}(k) + e^{-\frac{\Omega}{T\Omega}} \rho_{eff,2}^{\pm}(k), \quad (51)$$

where

$$\begin{aligned} \rho_{eff,1}^{\pm}(k) = & \alpha_k(a_\omega, a_\Omega) |k0^F\rangle \langle (k+1)1^{F+}| + \\ & + \beta_k(a_\omega, a_\Omega) |(k+1)0^F\rangle \langle (k+1)0^F| + \\ & + \delta_k(a_\omega, a_\Omega) |k1^{F+}\rangle \langle k1^{F+}| + \\ & + \gamma_k(a_\omega, a_\Omega) |(k+1)1^{F+}\rangle \langle k0^F| \end{aligned} \quad (52)$$

and

$$\begin{aligned} \rho_{eff,2}^{\pm}(k) = & \alpha_k(a_\omega, a_\Omega) |k1^{F-}\rangle \langle (k+1)1^{F+}1^{F-}| + \\ & + \beta_k(a_\omega, a_\Omega) |(k+1)1^{F-}\rangle \langle (k+1)1^{F-}| + \\ & + \delta_k(a_\omega, a_\Omega) |k1^{F+}1^{F-}\rangle \langle k1^{F+}1^{F-}| + \\ & + \gamma_k(a_\omega, a_\Omega) |(k+1)1^{F+}1^{F-}\rangle \langle k1^{F-}|, \end{aligned} \quad (53)$$

where we denoted $|n_\omega\rangle_I \otimes |0_\Omega\rangle_I^+ \otimes |0_\Omega\rangle_I^-$ by $|n0^F\rangle$, $|n_\omega\rangle_I \otimes |1_\Omega\rangle_I^+ \otimes |0_\Omega\rangle_I^-$ by $|n1^{F+}\rangle$, $|n_\omega\rangle_I \otimes |0_\Omega\rangle_I^+ \otimes |1_\Omega\rangle_I^-$ by $|n1^{F-}\rangle$ and $|n_\omega\rangle_I \otimes |1_\Omega\rangle_I^+ \otimes |1_\Omega\rangle_I^-$ by $|n1^{F+}1^{F-}\rangle$. Thus, if the fermionic mode is not accelerated, $\delta_k = 0$ and Φ_{BF}^\pm is entangled for all finite accelerations. We see that the effective density matrix (51) splits into two contributions. Further, it is easy to see that (52) and (53) carry the same entanglement. Therefore, in the following, we restrict ourself to $\rho_{eff,1}^{\pm}(k)$.

Similarly to the bosonic Φ^\pm -state, $\alpha_0 = \beta_0 = \gamma_0 = \delta_0 \neq 0$ for $a_\omega, a_\Omega < \infty$ is achieved due to the special structure of the reduced density matrix ρ_{BF}^\pm (cf. (C10)). For the further sectors, $k > 0$, $\alpha_k \gamma_k = \beta_k \delta_k \neq 0$ is enabled. For vanishing acceleration there are the initially non-vanishing coherences $|00^F\rangle \langle 11^{F+}|$ and $|11^{F+}\rangle \langle 00^F|$ that decrease with increasing acceleration. By increasing the acceleration some coherences are created ($|k0^F\rangle \langle (k+1)1^{F+}|$ and $|(k+1)1^{F+}\rangle \langle k0^F|$) and, further, the term $\frac{1}{2} \cos^4(r_f) a_n^2 (|n0^F\rangle \langle n0^F| + \tan^2(r_f) |n1^{F+}\rangle \langle n1^{F+}|)$ in (C10) leads to an increasing occupation of $|k1^{F+}\rangle \langle k1^{F+}|$ and $|(k+1)0^F\rangle \langle (k+1)0^F|$. In contrast to the bosonic Φ^\pm -state, this does not happen symmetrically. But at some point, when r and r_f fulfil $n_B^\omega n_F^\Omega = 1$, there is an occupation of these two states such that $\alpha_k \gamma_k = \beta_k \delta_k \neq 0$ and entanglement vanishes.

Furthermore, as for the bosonic Φ^\pm -state, the term $\frac{1}{2} \cos^2 \bar{a}_n^2 |(n+1)1^{F+}\rangle \langle (n+1)1^{F+}|$ as well as $\frac{1}{2} \sin^2(r_f) \cos^2(r_f) a_n^2 |n1^{F+}\rangle \langle n1^{F+}|$ contribute to the occupation of $|(k+1)0^F\rangle \langle (k+1)0^F|$ and therefore compensate part of the loss of occupation of that state that is caused by acceleration. Above we called this ‘‘diagonal mixing’’. This mixing enables $\alpha_k \gamma_k = \beta_k \delta_k \neq 0$ and therefore entanglement vanishes for finite accelerations.

Again we want to emphasize the dependence on the energy of the entangled modes. The condition for entanglement can be written as

$$n_B^\omega n_F^\Omega \leq 1. \quad (54)$$

This is equivalent to $\gamma_{\Phi_{BF}^\pm} \geq 0$. As in Section III, we see that entanglement is more persistent for higher frequency modes. Furthermore, we note that, for equal accelerations ($a_\omega = a_\Omega$), condition (54) can be written in terms of the Helmholtz free energies as

$$\omega + \Omega \geq T (\log(Z_B^\omega) - \log(Z_F^\Omega)) = -F_\omega + F_\Omega, \quad (55)$$

where $F_{\omega/\Omega}$ denote the Helmholtz free energies. Comparing that condition to (39), we see a huge similarity, as (39) can be written as $\omega + \Omega \geq -F_\omega - F_\Omega$. If we would take these equations for more than just a nice rewriting, we could conjecture that the origin of the non-vanishing entanglement for fermions is given by the fact that the condition for entanglement is $\omega + \Omega \geq F_\omega + F_\Omega$, where $F_\omega + F_\Omega \leq 0$, and thus it is trivially fulfilled for all accelerations.

To summarize, the negativities of states X_1 and X_2 factorize and we observe a product structure similar to the one obtained in Section III, where the total negativity is the product of the fermion and the boson contributions. That is due to the structure of the fermion mode Ω . These families of states are entangled for all finite accelerations. The negativities are given by the product of inverse bosonic and fermionic partition functions and therefore vanish in the limit of infinite acceleration. In case of the Φ^\pm and Ψ^\pm states (Φ_{BF}^\pm and Ψ_{BF}^\pm) this does not hold any more and we observe a behavior that is similar to the one we obtained for the Φ^\pm and Ψ^\pm states in Section IV. Again state Φ_{BF}^\pm loses all its entanglement for finite accelerations, while state Ψ_{BF}^\pm is entangled for all finite accelerations, see Figure 5. The different behavior is due to the different structures of the states, since only in the case of state Φ_{BF}^\pm diagonal mixing is enabled.

So, we have seen that, for fermion-fermion, boson-boson as well as for the boson-fermion Bell states, the degradation of entanglement does not depend on, for example, whether the state is a singlet or triplet, but on the structure of the particular state. It is the structure of the state that determines the fading of its entanglement.

In the following Section, we summarize our findings and discuss the role of particle statistics in the degradation of entanglement.

VI. ENTANGLEMENT DEGRADATION AND THE ROLE OF PARTICLE STATISTICS

In this Section we discuss the mechanisms behind entanglement degradation and the role of particle statistics therein. Above we discussed the fermion-fermion Bell states (16), the boson-boson Bell states (31) and the boson-fermion Bell states (45). Using the expressions for the negativities (21), (20), (32), (33) as well as (48), (49), we can write the negativities of all Bell states in the following compact form

$$N_{S_{XY}^\pm}^{(0)} = \frac{1}{2} \frac{1}{(Z_X^\omega)^x} \frac{1}{(Z_Y^\Omega)^y} \gamma_{S_{XY}^\pm}, \quad (56)$$

where $S_{XY}^\pm = \Psi_{XY}^\pm$, Φ_{XY}^\pm denotes the entangled state, X, Y encode the statistics of the fields (fermionic, bosonic) and x, y are equal to 1 for fermions ($X, Y = F$) and are equal to 2 for bosons ($X, Y = B$). The functions $\gamma_{S_{XY}^\pm}$ are given by

$$\gamma_{\Psi_{BB}^\pm} = \sqrt{Z_B^\omega Z_B^\Omega + \bar{n}_B^2 - \bar{n}_B}, \quad (57a)$$

$$\gamma_{\Psi_{BF}^\pm} = 1, \quad (57b)$$

$$\gamma_{\Psi_{FF}^\pm} = \sqrt{Z_F^\omega Z_F^\Omega + (Z_F^\omega Z_F^\Omega)^2 \bar{n}_F^2 - Z_F^\omega Z_F^\Omega \bar{n}_F} \quad (57c)$$

for the Ψ_{XY}^\pm states, where $\bar{n}_{B/F} = \frac{1}{2}(n_{B/F}^\omega + n_{B/F}^\Omega)$ is the average occupation number, and

$$\gamma_{\Phi_{BB}^\pm} = 1 - n_B^\omega n_B^\Omega, \quad (58a)$$

$$\gamma_{\Phi_{BF}^\pm} = \sqrt{\frac{n_B^\omega}{n_F^\Omega}} - n_B^\omega, \quad (58b)$$

$$\gamma_{\Phi_{FF}^\pm} = 1 \quad (58c)$$

for the Φ_{XY}^\pm states. Equation (56) gives the negativities in the $k = 0$ sector, where entanglement is initiated. For some states there is entanglement dynamically created in other sectors but these are always bounded from above by (56), see Figure 8 in the Appendix. Therefore these negativities capture the main features of entanglement degradation and we restrict our attention to these.

Physically speaking, after fixing the frequencies ω and Ω , as seen by the accelerated observers, equation (56) gives the negativity of the two-parameter family of states S_{XY}^\pm . That is, for each choice of the pair (a_ω, a_Ω) , equation (56) gives the negativity of the particular state S_{XY}^\pm that is characterized by $(\omega, \Omega, a_\omega, a_\Omega)$, when this state is seen by accelerated observers of accelerations a_ω and a_Ω , respectively. For this reason, and also because the Unruh modes that are considered are global modes, the setting should be considered as a toy model that captures the essential features of entanglement degradation.

There are essentially two factors determining the fading of entanglement. The first one is given by the set of states (as above, by states we mean diagonal elements of the density matrix) that become available when a state is accelerated. This set depends heavily on the structure of the state, as, for example, for Ψ^\pm the state $|00\rangle\langle 00|$ never becomes accessible, but also on the statistics that does not allow for two- or more-particle states for fermions. The second determining factor is whether the population of states $|00\rangle\langle 00|$, $|01\rangle\langle 01|$, $|10\rangle\langle 10|$ and $|11\rangle\langle 11|$ can be transferred completely to higher excited states like, for example, $|21\rangle\langle 21|$. If that is possible also the coherences $|00\rangle\langle 11|$ and $|01\rangle\langle 10|$ vanish with increasing acceleration. Both factors depend heavily on the statistics of the underlying field.

For illustrating reasons consider the following density

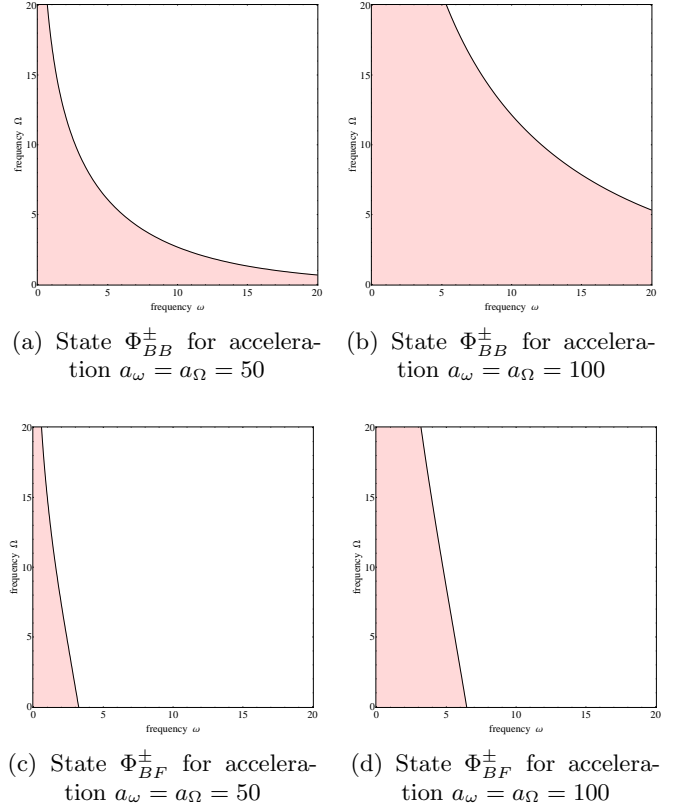


FIG. 6: Energy dependence of the entanglement in Bell states $\Phi_{BB/BF}^\pm$: States of modes of energies ω and Ω contained in the red region show no entanglement, while states of higher energies remain entangled (white region). The plots show states $\Phi_{BB/BF}^\pm$ for acceleration $a_\omega = a_\Omega = 50$ ((a), (c)) and $a_\omega = a_\Omega = 100$ ((b), (d)). State Φ_{FF}^\pm is entangled for all frequencies and accelerations and therefore it is not shown. The zeros of the functions $\gamma_{\Phi_{BB}^\pm}$ and $\gamma_{\Phi_{BF}^\pm}$ define the border between the regions. The asymmetry in (c) and (d) is due to the fact that fermions are “more resistant” towards the effects of acceleration.

matrix ρ

$$\rho = \begin{pmatrix} \rho_{0000}^\Phi & 0 & 0 & \rho_{0011}^\Phi \\ 0 & \rho_{0101}^\Psi & \rho_{0110}^\Psi & 0 \\ 0 & \rho_{1001}^\Psi & \rho_{1010}^\Psi & 0 \\ \rho_{1100}^\Phi & 0 & 0 & \rho_{1111}^\Phi \end{pmatrix} \quad (59)$$

written in the basis $\{|00\rangle, |01\rangle, |10\rangle, |11\rangle\}$, where all ρ_{ijkl}^Φ ($i, j, k, l \in \{0, 1\}$) are zero for Ψ^\pm states and vice versa. Tracing out anti-particles, (59) is the full density matrix for fermions and acceleration decreases the diagonal elements ($\rho_{0000}^\Phi, \rho_{1111}^\Phi; \rho_{0101}^\Psi, \rho_{1010}^\Psi$) as well as the coherences ($\rho_{0011}^\Phi, \rho_{1100}^\Phi; \rho_{1001}^\Psi, \rho_{0110}^\Psi$) to a finite value for both Φ^\pm and Ψ^\pm states. Furthermore, the “squared” coherences $\rho_{0011}^\Phi \rho_{1100}^\Phi$ and $\rho_{1001}^\Psi \rho_{0110}^\Psi$ always dominate the product of the occupations of states $\rho_{0000}^\Phi, \rho_{1111}^\Phi$ and $\rho_{0101}^\Psi, \rho_{1010}^\Psi$, respectively. That is why entanglement decreases but does

not vanish.

For bosons, in contrast, (59) is only the initially non-vanishing part of the infinite dimensional density matrix. The reason why Φ^\pm states lose their entanglement (cf. Figure 6), while Ψ^\pm are entangled for all finite accelerations, is given by the set of available states (cf. Sections IV and V). The reason for the asymptotic vanishing of the negativity for all boson-boson and boson-fermion states is given by the second determining factor (see above). All initially non-vanishing elements of ρ , i.e. the ρ_{ijkl}^Φ and the ρ_{ijkl}^Ψ , approach zero in the infinite acceleration limit, as matrix elements of higher excitation states are increasing. That is due to bosonic statistics. Naively fermions get “rotated” and bosons “smeared” towards higher excited sectors due to acceleration. Furthermore, note the asymmetry in Figure 6 that is due to the fact that fermions are “more resistant” towards the effects of acceleration.

This explanation based on the two determining factors captures the role of particle statistics. Particle statistics also is reflected in the negativities (56) that are written in terms of the partition functions and the occupation numbers and therefore make the “effects of statistics” apparent.

In this work we studied maximally entangled states like, for example,

$$|\Psi_\alpha\rangle = \sin(\alpha)|0_\omega\rangle_U|1_\Omega\rangle_U + \cos(\alpha)|1_\omega\rangle_U|0_\Omega\rangle_U, \quad (60a)$$

$$|\Phi_\alpha\rangle = \sin(\alpha)|0_\omega\rangle_U|0_\Omega\rangle_U + \cos(\alpha)|1_\omega\rangle_U|1_\Omega\rangle_U, \quad (60b)$$

where we chose α to be $\pi/4$. Differing choices of α lead to less entangled states, as the negativity $N_{\Psi_\alpha} = N_{\Phi_\alpha} = \sin(\alpha)\cos(\alpha)$ is maximized for $\alpha = \pi/4$. Given the mechanisms that lead to entanglement degradation that we outlined above, it is evident that states (60) behave qualitatively the same for generic α as they do for $\alpha = \pi/4$, i.e. in the maximally entangled case. In the case of more general mixed states, we expect that, depending on the state, one observes that the degradation of entanglement shows characteristics that are best described by a mixture of the characteristics of the degradations in the case of Φ^\pm and Ψ^\pm . But it seems reasonable to expect that a random mixed state will lose its entanglement for finite acceleration with high probability, as in the fermionic case studied in [41].

In some sense we can think of the functions γ ((57) and (58)) as deformations of an (universal) particle statistics dependent negativity \mathcal{N}_U

$$\mathcal{N}_U = \frac{1}{2} \frac{1}{(Z_X^\omega)^x} \frac{1}{(Z_Y^\Omega)^y} \quad (61)$$

that only depends on the partition functions that are characteristic for the particle statistics of the field. Then the particular structure of the Bell state, as well as the particle statistics, set the γ that we might call structure functions and denote them by $\gamma_{structure}$. As we saw, these depend heavily on the set of states whose occupation is driven by the Unruh effect. So finally we can write

the entanglement of a Bell state (negativity N_{state}) in the sector where entanglement is initialized as

$$N_{state} = \gamma_{structure} \mathcal{N}_U. \quad (62)$$

We want to close this Section by giving some comments on equation (62). First, choosing the partitioning of N_{state} in $\gamma_{structure}$ and \mathcal{N}_U is not unique and there are possible partitions different from (56). Nevertheless writing the negativity in form (62) makes the importance of the particular structure of the state manifest. Moreover, equation (62) allows to clearly identify the two determining factors: The first one sets the function $\gamma_{structure}$, while the second one determines \mathcal{N}_U . Further, we note that a slightly varied form of (62) also holds for states X_1 and X_2 . We expect that there are slight modifications when there are different particles involved, like particles carrying spin. Finally, it would be interesting to figure out whether the negativities of non-maximally entangled mixed states could also be captured in an expression similar to (62).

In the following Section, we point out possible implications of above findings for particles in Bell states close to the black hole horizon.

VII. DEGRADATION OF ENTANGLEMENT IN THE VICINITY OF A BLACK HOLE

The framework we used in this work also applies to the spacetime close to a black hole, as outlined in Appendix D (see also [19]). But given the caveats in the interpretation of the states, we described in Section III, the following discussion is more of speculative nature and aims at giving a qualitative idea about entanglement degradation near black holes.

One point that can be inferred is that entanglement gets degraded in the vicinity of the black hole horizon. Further, all states that involve bosons lose their entanglement in the limit of reaching the horizon. This is in contrast to the fermion-fermion states, where entanglement never vanishes. Further there are crucial differences between the degradation of entanglement for states Φ^\pm and Ψ^\pm . The entanglement of states Φ_{BB}^\pm and Φ_{BF}^\pm completely vanishes at a finite distance from the horizon that is large compared to the Planck length L_P ($d \approx 0.01 R_S$, where R_S is the Schwarzschild radius), whereas states Ψ^\pm are entangled for any finite distance from the black hole.

Thus, we observed that entanglement, an important resource for quantum information tasks, gets degraded very differently for differing Bell states, i.e. the degradation of entanglement is state dependent. Our findings imply that there are particular states that remain entangled as seen by an observer that is uniformly accelerated or equivalently is stationary close to a black hole, while, for other choices of the state, there is no entanglement remaining. Although, these considerations are rather speculative, given the fact that we are not describing the en-

tanglement of a fixed state for different accelerations but for each acceleration there is a different state (cf. Section III), they still qualitatively capture the main features of entanglement degradation near a black hole. In the light of the Black Hole Information Paradox [43, 44], it would be interesting to see whether a similar phenomenon also occurs in a more realistic localized approach as in [29–31]. Especially, the dependence on the particular structure of the state deserves further studies.

VIII. CONCLUSIONS

In this work, we studied families of two uniformly accelerated maximally entangled Unruh modes in the general case of different accelerations, and analysed their entanglement, measured by the negativity. Therefore, we considered states containing two fermionic modes, two bosonic modes, as well as states of one bosonic and one fermionic mode. Special emphasis was given to the comparison of Bell states Φ^\pm and Ψ^\pm . Although the Unruh modes we used do not have a simple physical interpretation, our studies provide insight into the mechanisms that lead to the degradation of entanglement due to acceleration.

We found that, in contrast to the other cases, purely fermionic families of Bell states are entangled for all accelerations. Still, the entanglement of state Ψ^\pm degrades faster with acceleration than the entanglement of state Φ^\pm . Interestingly, it is only for state Ψ^\pm that both accelerated modes give rise to a contribution to the same diagonal element of the reduced density matrix that is relevant for entanglement. We suspect that this special feature of Ψ^\pm is responsible for the different behavior regarding entanglement degradation. Furthermore, we found that also classical correlations are partially lost due to acceleration.

In the purely bosonic case, as well as in the boson-fermion case, state Ψ^\pm remains entangled for all finite accelerations, and entanglement vanishes asymptotically in the limit of infinite accelerations. In contrast, state Φ^\pm loses its entanglement for some finite acceleration. This is manifest in the presence of a “cut off function” γ_{Φ^\pm} in the expression for the negativity. So we found that the type of Bell state (i.e. being Φ^\pm or Ψ^\pm) crucially affects the robustness of its entanglement against acceleration. Furthermore, we obtained that the reason for the occurrence of this phenomenon is originated in the particular occupation patterns of the constituents (the “structure”) of the state, that determine which excitations can be driven by the Unruh effect.

Applying an effective state picture, we were able to explain this crucial difference between both types of states. State Ψ^\pm is entangled for all finite accelerations as the Unruh effect does not drive the occupation of state $|00\rangle\langle 00|$, and this state is naturally absent in the density matrix of Ψ^\pm . Entanglement vanishes only asymptotically for infinite acceleration, as in this regime all occu-

pation is shifted towards highly excited states. For state Φ^\pm things are different. Essentially what happens is the following. For vanishing acceleration, there exist the coherences $|00\rangle\langle 11|$ and $|11\rangle\langle 00|$ that are responsible for the entanglement, while the occupation of $|10\rangle\langle 10|$ and $|01\rangle\langle 01|$ is vanishing. When acceleration is increasing, the coherences are decreasing, while at the same time the occupation of $|10\rangle\langle 10|$ and $|01\rangle\langle 01|$ is driven (symmetrically) by the Unruh effect by creating one excitation in $|00\rangle\langle 00|$. Thus, for the value of the acceleration for which the condition for entanglement (cf. (38), (54)) is violated, entanglement vanishes. Hence, we traced the difference in the behavior regarding entanglement degradation back to the set of accessible states and the symmetry in the distribution of probability amongst them. It seems that diagonal mixing, as we coined it above, is required to achieve sufficient uniformity in the occupation of the states.

Further, we found that there are two factors that determine the fading of entanglement. The first one, given by the set of states that become accessible due to the Unruh effect, is heavily influenced by the structure of the state. Said factor determines whether a state loses its entanglement for finite accelerations or not. The second factor is more closely related to the particle statistics of the modes that constitute the Bell state. It is whether higher excitation states become accessible due to acceleration or not. That is the case for bosonic modes, and thus Bell states in which these modes are involved are non-entangled in the infinite acceleration limit, whereas purely fermionic Bell states are always entangled. Remarkably, we found that the negativities of the boson-boson, boson-fermion and fermion-fermion Bell states can be expressed in the same form (56)

$$N_{S_{XY}^\pm}^{(0)} = \frac{1}{2} \frac{1}{(Z_X^\omega)^x} \frac{1}{(Z_Y^\omega)^y} \gamma_{S_{XY}^\pm}, \quad (63)$$

where the $Z_{B/F}^{\omega/\Omega}$ are the partition functions (of a harmonic oscillator/two-level system with energy gap ω/Ω) and the $\gamma_{S_{XY}^\pm}$ are functions determined by the first factor, we introduced above.

Furthermore, we discussed possible effects of hovering over a black hole on entangled states of two Unruh modes.

In summary, our studies reveal the mechanisms that cause the behavior of entanglement in accelerated frames to depend heavily on the particular occupation patterns of the constituents of the entangled state.

ACKNOWLEDGMENTS

We would like to thank Dieter Lüst for useful discussions and Andrzej Dragan for comments and bringing references [29–31] to our attention. Further we thank the support from Fundação para a Ciência e a Tecnologia (Portugal), namely through

programmes PTDC/POPH and projects PESTOE/EGE/UI0491/2013, UID/EEA/50008/2013, IT/QuSim and CRUP-CPU/CQVibes, partially funded by EU FEDER, and from the EU FP7 projects LANDAUER (GA 318287) and PAPETS (GA 323901). BR acknowledges the support from the DP-PMI and FCT (Portugal) through scholarship SFRH/BD/52651/2014.

Appendix A: Fermion-fermion states

1. Calculation of negativities

We give more details of the calculations of the negativities of the fermion states. The calculation of the negativity (19) requires the partially transposed reduced density matrices ρ_i^{pT} of states (16). We obtain the density matrices according to (17) and by tracing out region II we end up with the reduced density matrices of the fermion states ρ_i . Finally, by partial transposition (let $\rho = \sum_{ijkl} p_{ijkl} |i\rangle\langle j| \otimes |k\rangle\langle l|$ then $\rho^{pT} = \sum_{ijkl} p_{ijkl} |i\rangle\langle j| \otimes |l\rangle\langle k|$ is the partial transposed) we obtain the ρ_i^{pT} . These are block diagonal. In case of state Φ_{FF}^\pm the part of $\rho_{\Phi_{FF}^\pm}^{pT}$ that gives rise to negative eigenvalues is of the following block diagonal form

$$\begin{pmatrix} 1 & 0 & 0 & 0 \\ 0 & \tan^2(r_f^\omega) & 0 & 0 \\ 0 & 0 & \tan^2(r_f^\Omega) & 0 \\ 0 & 0 & 0 & \tan^2(r_f^\omega) \tan^2(r_f^\Omega) \end{pmatrix} \otimes \rho_{(\Phi_{FF}^\pm)}^{pT}, \quad (\text{A1})$$

where \otimes denotes the Kronecker product and

$$\begin{aligned} \rho_{(\Phi_{FF}^\pm)}^{pT} &= \frac{1}{2} \cos^2(r_f^\omega) \cos^2(r_f^\Omega) \times \\ &\times \begin{pmatrix} \sin^2(r_f^\omega) \cos^2(r_f^\Omega) & \cos(r_f^\omega) \cos(r_f^\Omega) \\ \cos(r_f^\omega) \cos(r_f^\Omega) & \sin^2(r_f^\Omega) \cos^2(r_f^\omega) \end{pmatrix}. \end{aligned} \quad (\text{A2})$$

Calculating the negative eigenvalues of (A1) the negativity $N_{\Phi_{FF}^\pm}$ can be expressed as

$$\begin{aligned} N_{\Phi_{FF}^\pm} &= (1 + \tan^2(r_f^\omega) + \tan^2(r_f^\Omega) + \tan^2(r_f^\omega) \tan^2(r_f^\Omega)) \times \\ &\times N(\rho_{(\Phi_{FF}^\pm)}^{pT}) \\ &= \frac{1}{2} \cos^2(r_f^\omega) \cos^2(r_f^\Omega). \end{aligned} \quad (\text{A3})$$

Moving to state Ψ_{FF}^\pm , we see that the part of $\rho_{\Psi_{FF}^\pm}^{pT}$ that gives rise to negative eigenvalues is of the same form as (A1), but this time $\rho_{(i)}^{pT}$ is of different structure. There is one element that has the form of a sum of contributions

of the two different modes. $\rho_{(\Psi_{FF}^\pm)}^{pT}$ is given by

$$\begin{aligned} \rho_{(\Psi_{FF}^\pm)}^{pT} &= \frac{1}{2} \cos^2(r_f^\omega) \cos^2(r_f^\Omega) \\ &\times \begin{pmatrix} 0 & \cos(r_f^\omega) \cos(r_f^\Omega) \\ \cos(r_f^\omega) \cos(r_f^\Omega) & \sin^2(r_f^\omega) + \sin^2(r_f^\Omega) \end{pmatrix} \end{aligned} \quad (\text{A4})$$

and $N_{\Psi_{FF}^\pm}$ is

$$\begin{aligned} N_{\Psi_{FF}^\pm} &= (1 + \tan^2(r_f^\omega) + \tan^2(r_f^\Omega) + \tan^2(r_f^\omega) \tan^2(r_f^\Omega)) \times \\ &\times N(\rho_{(\Psi_{FF}^\pm)}^{pT}) \\ &= \frac{1}{4} (-(\sin^2(r_f^\omega) + \sin^2(r_f^\Omega)) + \\ &+ \sqrt{(\sin^2(r_f^\omega) + \sin^2(r_f^\Omega))^2 + 4 \cos^2(r_f^\omega) \cos^2(r_f^\Omega)}). \end{aligned} \quad (\text{A5})$$

In our calculations we considered that both observers are able to detect and to distinguish particles and anti-particles. Therefore, we obtained the density matrices ρ_i to be 16×16 -matrices. But we want to note that, due to the structure of (A1), the negativities are given by the same expressions, when we assume that only particles can be detected and therefore trace out anti-particles. In this case, we end up with ρ_i being 4×4 -matrices (like in the case of two qubits).

2. Entanglement in different sectors

We briefly discuss the distribution of entanglement in states ψ_i , when the acceleration is non-vanishing. Considering (A1) we see that, while entanglement in the sector where it was initiated is decreasing with increasing acceleration, there is entanglement created in previously non-entangled sectors. Schematically we can write $N_{\Phi_{FF}^\pm}$ as

$$\begin{aligned} N_{\Phi_{FF}^\pm} &= N(0, 0 | 1^+, 1^+) \\ &+ N(1^-, 0 | 1^+ 1^-, 1^+) \\ &+ N(0, 1^- | 1^+, 1^+ 1^-) \\ &+ N(1^-, 1^- | 1^+ 1^-, 1^+ 1^-), \end{aligned} \quad (\text{A6})$$

where

$$N(0, 0 | 1^+, 1^+) = N(\rho_{(\Phi_{FF}^\pm)}^{pT}), \quad (\text{A7})$$

$$N(1^-, 0 | 1^+ 1^-, 1^+) = \tan^2(r_f^\omega) N(\rho_{(\Phi_{FF}^\pm)}^{pT}), \quad (\text{A8})$$

$$N(0, 1^- | 1^+, 1^+ 1^-) = \tan^2(r_f^\Omega) N(\rho_{(\Phi_{FF}^\pm)}^{pT}), \quad (\text{A9})$$

$$N(1^-, 1^- | 1^+ 1^-, 1^+ 1^-) = \tan^2(r_f^\omega) \tan^2(r_f^\Omega) N(\rho_{(\Phi_{FF}^\pm)}^{pT}) \quad (\text{A10})$$

are the negativities of the different sectors. $N(0, 0 | 1^+, 1^+)$ is the negativity of the sector,

where the entanglement is initialized, i.e. entanglement between $|0_\omega\rangle_I^+ \otimes |0_\omega\rangle_I^- \otimes |0_\Omega\rangle_I^+ \otimes |0_\Omega\rangle_I^-$ and $|1_\omega\rangle_I^+ \otimes |0_\omega\rangle_I^- \otimes |1_\Omega\rangle_I^+ \otimes |0_\Omega\rangle_I^-$. There are three sectors in which entanglement is created due to acceleration (A8)-(A10). The negativities are plotted in Figure 7 and we see that the entanglement is distributed equally between the sectors in the infinite acceleration limit.

For state Ψ_{FF}^\pm we see again, that entanglement is created in some sectors and we can write $N_{\Psi_{FF}^\pm}$ schematically as

$$\begin{aligned} N_{\Psi_{FF}^\pm} = & N(1^+, 0 | 0, 1^+) \\ & + N(1^+ 1^-, 0 | 1^-, 1^+) \\ & + N(1^+, 1^- | 0, 1^+ 1^-) \\ & + N(1^+ 1^-, 1^- | 1^-, 1^+ 1^-), \end{aligned} \quad (\text{A11})$$

where

$$N(1^+, 0 | 0, 1^+) = N(\rho_{(\Psi_{FF}^\pm)}^{pT}), \quad (\text{A12})$$

$$N(1^+ 1^-, 0 | 1^-, 1^+) = \tan^2(r_f^\omega) N(\rho_{(\Psi_{FF}^\pm)}^{pT}), \quad (\text{A13})$$

$$N(1^+, 1^- | 0, 1^+ 1^-) = \tan^2(r_f^\Omega) N(\rho_{(\Psi_{FF}^\pm)}^{pT}), \quad (\text{A14})$$

$$N(1^+ 1^-, 1^- | 1^-, 1^+ 1^-) = \tan^2(r_f^\omega) \tan^2(r_f^\Omega) N(\rho_{(\Psi_{FF}^\pm)}^{pT}) \quad (\text{A15})$$

are the negativities of the different sectors. $N(1^+, 0 | 0, 1^+)$ is the negativity of the sector, where the entanglement is initialized. When the acceleration increases from zero the negativity $N(1^+, 0 | 0, 1^+)$ decreases while (A13)-(A15) increase. In the infinite acceleration limit all sectors are equally entangled, see Figure 7. Comparing states Φ_{FF}^\pm and Ψ_{FF}^\pm , we note that the “redistribution” of entanglement is the same for small accelerations, but differs more and more with increasing acceleration, until finally different limiting values are approached.

We plot the entanglement in the sectors that show creation of entanglement in Figure 7. This effect is due to a symmetric production of particle-antiparticle pairs. We can, for example, write state Φ_{FF}^\pm schematically as $0, 0 | 1^+, 1^+$. Then, for non-zero acceleration, the Unruh effect, that in some sense can be seen as pair production, populates states $0, 1^-$ and $1^+, 1^+ 1^-$ and thus creates entanglement ($N(0, 1^- | 1^+, 1^+ 1^-) \neq 0$) in the sector $0, 1^- | 1^+, 1^+ 1^-$. In the same manner there is entanglement created in the sectors $1^-, 0 | 1^+ 1^-, 1^+$ and $1^-, 1^- | 1^+ 1^-, 1^+ 1^-$, see Figure 7. But, in general, not all states show this behavior. One state that does not show this feature is $\frac{1}{\sqrt{2}}(|1_\omega^F\rangle_U |1_\Omega^F\rangle_U + |1_\omega^F\rangle_U |1_\Omega^F\rangle_U)$. The reason why there is no entanglement generated is that for this state symmetric pair production would require a violation of the Pauli Principle and therefore is forbidden.

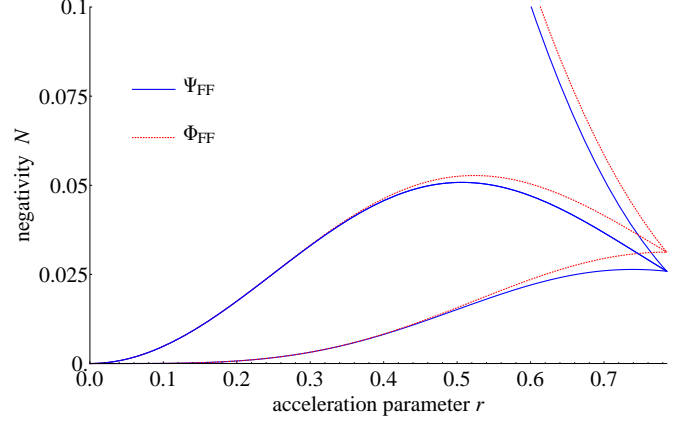


FIG. 7: Entanglement distribution for states Φ_{FF}^\pm (red, dotted) and Ψ_{FF}^\pm (blue) plotted versus the acceleration parameter $r = r_f^\omega = r_f^\Omega$. The infinite acceleration limit corresponds to $r = \frac{\pi}{4}$. The middle pair of solid curves is twofold degenerate due to the symmetry of the states. With increasing acceleration, entanglement is created in previously separable sectors. From top to bottom the curves correspond to: red: $N(0, 0 | 1^+, 1^+)$, $N(1^-, 0 | 1^+ 1^-, 1^+)$ and $N(0, 1^- | 1^+, 1^+ 1^-)$, $N(1^-, 1^- | 1^+ 1^-, 1^+ 1^-)$; blue: $N(1^+, 0 | 0, 1^+)$, $N(1^+ 1^-, 0 | 1^-, 1^+)$ and $N(1^+, 1^- | 0, 1^+ 1^-)$, $N(1^+ 1^-, 1^- | 1^-, 1^+ 1^-)$.

3. Rényi-2 entropies

The Rényi-2 entropies (28) are given in the following. For convenience we carry out the calculations for $r^\omega = r^\Omega = r$. Due to the relative simplicity, we are able to find compact analytical expressions for the Rényi-2 entropies of states (16)

$$S_2(\rho_{\Phi_{FF}^\pm}) = -\log\left(\frac{(20\cos(4r) + \cos(8r) + 43)^2}{4096}\right), \quad (\text{A16a})$$

$$S_2(\rho_{\Psi_{FF}^\pm}) = -3\log(\sin^4(r) + \cos^4(r)) \quad (\text{A16b})$$

and we find the infinite acceleration limits

$$S_2^\infty(\rho_{\Phi_{FF}^\pm}) = \log\left(\frac{64}{9}\right), \quad (\text{A17a})$$

$$S_2^\infty(\rho_{\Psi_{FF}^\pm}) = \log(8). \quad (\text{A17b})$$

Appendix B: Boson-boson states

We calculate the negativity (19) for the following bosonic Bell states

$$|\Psi_{BB}^\pm\rangle = \frac{1}{\sqrt{2}}(|0_\omega\rangle_U |1_\Omega\rangle_U \pm |1_\omega\rangle_U |0_\Omega\rangle_U), \quad (\text{B1a})$$

$$|\Phi_{BB}^\pm\rangle = \frac{1}{\sqrt{2}}(|0_\omega\rangle_U |0_\Omega\rangle_U \pm |1_\omega\rangle_U |1_\Omega\rangle_U), \quad (\text{B1b})$$

where ω, Ω are the frequencies and 0, 1 the occupation numbers of the Unruh-modes. The two modes ω and Ω undergo constant accelerations a_ω and a_Ω . The acceleration parameters of the modes are denoted by r^ω and r^Ω , respectively.

We start with state Φ_{BB}^\pm and for concreteness we consider Φ_{BB}^+ that shows the same entanglement as Φ_{BB}^\pm . So in the following we will always denote Φ_{BB}^+ by Φ_{BB}^\pm and similarly for the Ψ^\pm states. The density matrix $\rho_{\Phi_{BB}^\pm}$ that we obtain after tracing out region II is given by

$$\begin{aligned} \rho_{\Phi_{BB}^\pm} &= \frac{1}{2} \sum_{m,n} a_m^2 a_n^2 |nm\rangle \langle nm| \\ &+ \frac{1}{2} \sum_{m,n} \bar{a}_m^2 \bar{a}_n^2 |(n+1)(m+1)\rangle \langle (n+1)(m+1)| \\ &+ \frac{1}{2} \sum_{m,n} a_m a_n \bar{a}_m \bar{a}_n |nm\rangle \langle (n+1)(m+1)| + h.c., \end{aligned} \quad (B2)$$

where $|nm\rangle = |n_\omega\rangle_I \otimes |m_\Omega\rangle_I$ and $a_n = a_n(r^\omega) = \tanh^n(r^\omega) \cosh^{-1}(r^\omega)$, $\bar{a}_n = \bar{a}_n(r^\omega) = \tanh^n(r^\omega) \cosh^{-2}(r^\omega) \sqrt{n+1}$. Accordingly, $a_m = a_{n=m}(r^\Omega)$ and $\bar{a}_m = \bar{a}_{n=m}(r^\Omega)$. The negativity can be obtained as a sum over the negativities for different values of n, m ($N_{\Phi_{BB}^\pm} = \sum_{n,m} N_{\Phi_{BB}^\pm}^{(n,m)}$). This can be seen from the block diagonal structure of the partially transposed density matrix. The part of the partially transposed density matrix that contributes to $N_{\Phi_{BB}^\pm}^{(n,m)}$ and the negativity $N_{\Phi_{BB}^\pm}$ are given by

$$\frac{1}{2} \frac{\tanh^{2n}(r^\omega) \tanh^{2m}(r^\Omega)}{\cosh^2(r^\omega) \cosh^2(r^\Omega)} \left(\left(1 + \frac{(m+1)n}{\sinh^2(r^\omega) \sinh^2(r^\Omega)} \right) \tanh^2(r^\Omega) \frac{\sqrt{(m+1)(n+1)}}{\cosh(r^\omega) \cosh(r^\Omega)} \right. \\ \left. \left(1 + \frac{(n+1)m}{\sinh^2(r^\omega) \sinh^2(r^\Omega)} \right) \tanh^2(r^\omega) \right) \quad (B3)$$

and

$$\begin{aligned} N_{\Phi_{BB}^\pm} &= \sum_{n,m} N_{\Phi_{BB}^\pm}^{(n,m)} = \sum_n N_{\Phi_{BB}^\pm}^{(n,0)} + \sum_m N_{\Phi_{BB}^\pm}^{(0,m)} \\ &= N_{\Phi_{BB}^\pm}^{(0)} + \sum_{n=1}^{\infty} \frac{\tanh^{2n}(r^\omega)}{4 \cosh^2(r^\omega) \cosh^2(r^\Omega)} (\tanh^2(r^\omega) + \tanh^2(r^\Omega) + \frac{n}{\sinh^2(r^\omega) \cosh^2(r^\Omega)} + \\ &+ \frac{2}{\sinh^2(r^\omega) \sinh^2(r^\Omega) \cosh(r^\omega) \cosh(r^\Omega)} (\frac{n^2}{4} \cosh^2(r^\omega) \sinh^2(r^\Omega) \tanh^2(r^\Omega) + \sinh^4(r^\omega) \sinh^4(r^\Omega) \times \\ &\times (\frac{n}{2} + \frac{1}{4} \cosh^2(r^\omega) \sinh^2(r^\Omega) \tanh^2(r^\Omega) + 1) + \frac{n}{2} \sinh^2(r^\omega) \cosh^2(r^\omega) \sinh^4(r^\Omega) \tanh^2(r^\Omega) + \\ &+ \sinh^6(r^\omega) (\frac{1}{4} \tanh^2(r^\omega) \sinh^4(r^\Omega) \cosh^2(r^\Omega) - \frac{1}{2} \sinh^6(r^\Omega)))^{\frac{1}{2}}) + \sum_{m=1}^{\infty} (\omega \leftrightarrow \Omega; n \rightarrow m), \end{aligned} \quad (B4)$$

where we used that $N_{\Phi_{BB}^\pm}^{(n,m)} \neq 0$ only for either $n = 0$ or $m = 0$ or $n = m = 0$. It can be seen that each of the $N_{\Phi_{BB}^\pm}^{(n,m)}$ is bounded from above by $N_{\Phi_{BB}^\pm}^{(0)} \equiv N_{\Phi_{BB}^\pm}^{(0,0)}$ that describes the entanglement between the modes we initially start with. For non-vanishing acceleration there is entanglement created between higher modes, i.e. $N_{\Phi_{BB}^\pm}^{(n,m)} \neq 0$, but this will be a small contribution compared to $N_{\Phi_{BB}^\pm}^{(0)}$, see Figure 8a.

To obtain $N_{\Phi_{BB}^\pm}^{(0)}$, we set n and m to zero in (B3). The

negativity $N_{\Phi_{BB}^\pm}^{(0)}$ can be written in the following form

$$N_{\Phi_{BB}^\pm}^{(0)} = 2N_{0,\omega} N_{0,\Omega} \gamma_{\Phi_{BB}^\pm} (n_B^\omega, n_B^\Omega), \quad (B5)$$

where $n_B^{\omega/\Omega} = (e^{\frac{\omega/\Omega}{T_{\omega/\Omega}}} - 1)^{-1}$ is the Bose-Einstein distribution and $N_{0,\omega/\Omega}$ denotes the negativities if only mode ω/Ω are accelerated. These can be obtained from (B4) by setting the acceleration parameter $r^{\omega/\Omega}$ to zero

$$N_{\Phi_{BB}^\pm}^{(0)} (r^\omega, r^\Omega = 0) \equiv N_{0,\omega} = \frac{1}{2} \frac{1}{(Z_B^\omega)^2}, \quad (B6)$$

where $Z_B^{\omega/\Omega}$ is the bosonic partition function (14). Fur-

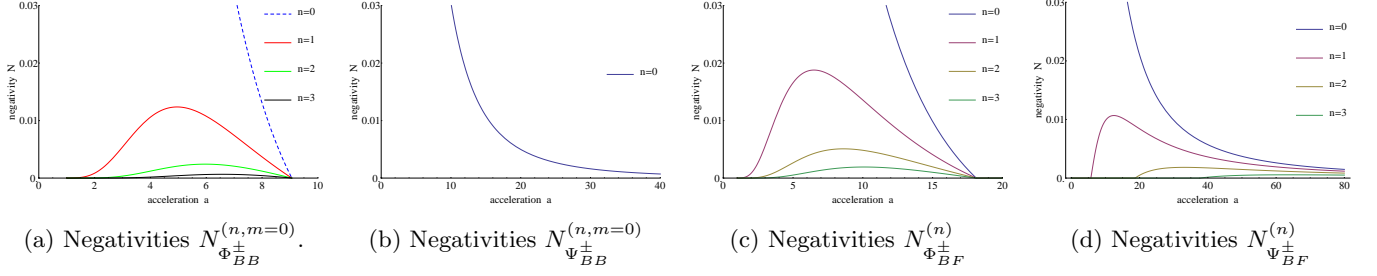


FIG. 8: Negativities, where both observers are accelerated, plotted against $a = a_{\omega} = a_{\Omega}$ for $\omega = 1$, $\Omega = 1$. While for states Φ_{BB}^{\pm} , Φ_{BF}^{\pm} and Ψ_{BF}^{\pm} there is entanglement created in initially non-entangled sectors (a), (c) and (d), there is no entanglement production (with this special choice of the acceleration parameter $r = r^{\omega} = r^{\Omega}$) for Ψ_{BB}^{\pm} (b).

Therefore in the generic case there is entanglement generated in initially non-entangled sectors.

ther $\gamma_{\Phi_{BB}^{\pm}}$ is given by

$$\gamma_{\Phi_{BB}^{\pm}} = 1 - n_B^{\omega} n_B^{\Omega}. \quad (\text{B7})$$

Now we move to state Ψ_{BB}^{\pm} , where the relevant part of the partially transposed reduced density matrix is given by the following expression

$$\frac{1}{2} \frac{\tanh^{2n}(r^{\omega}) \tanh^{2m}(r^{\Omega})}{\cosh^2(r^{\omega}) \cosh^2(r^{\Omega})} \left(\frac{\frac{m}{\sinh^2(r^{\Omega})} + \frac{n}{\sinh^2(r^{\omega})}}{\frac{\sqrt{(m+1)(n+1)}}{\cosh(r^{\omega}) \cosh(r^{\Omega})}} \quad \frac{\sqrt{(m+1)(n+1)}}{\cosh(r^{\omega}) \cosh(r^{\Omega})} \right). \quad (\text{B8})$$

Contrary to (B3), only the eigenvalues of the block ($n = 0, m = 0$) can be negative (Figure 8b) for $r^{\omega} = r^{\Omega}$. In this case, the sum of the partial negativities $N_{\Psi_{BB}^{\pm}} = \sum_{n,m} N_{\Psi_{BB}^{\pm}}^{(n,m)}$ collapses to $N_{\Psi_{BB}^{\pm}} = N_{\Psi_{BB}^{\pm}}^{(0)}$ and we find

$$N_{\Psi_{BB}^{\pm}}^{(0)} = \frac{1}{2} \frac{1}{(Z_B^{\omega})^2} \frac{1}{(Z_B^{\Omega})^2} \times \left(\sqrt{Z_B^{\omega} Z_B^{\Omega} + \frac{1}{4} (n_B^{\omega} + n_B^{\Omega})^2} - \frac{1}{2} (n_B^{\omega} + n_B^{\Omega}) \right). \quad (\text{B9})$$

In the case $r^{\omega} \neq r^{\Omega}$, we assume without loss of generality $r^{\omega} > r^{\Omega}$. Then the blocks for $m = 0$ admit negative eigenvalues and we find the negativity

$$N_{\Psi_{BB}^{\pm}} = N_{\Psi_{BB}^{\pm}}^{(0)} + \sum_{n=1}^{\infty} \frac{\tanh^{2n}(r^{\omega})}{4 \cosh^4(r^{\omega}) \cosh^4(r^{\Omega})} (-n \coth^2(r^{\omega}) \cosh^2(r^{\Omega}) - (n+1) \sinh^2(r^{\Omega}) - \sinh^2(r^{\omega}) + \frac{1}{\sinh^2(r^{\omega})} \left(\left(\frac{n}{2} \cosh(2r^{\omega}) \cosh(2r^{\Omega}) + \frac{n}{2} + \sinh^2(r^{\omega}) \sinh^2(r^{\Omega}) + \sinh^4(r^{\omega}) \right)^2 - \frac{1}{4} \sinh^2(2r^{\omega}) \sinh^2(2r^{\Omega}) (n(n+1) \sinh^4(r^{\Omega}) - \sinh^2(r^{\omega}) \sinh^2(r^{\Omega})) \right)^{\frac{1}{2}}), \quad (\text{B10})$$

where $N_{\Psi_{BB}^{\pm}}^{(0)}$ is given by (B9).

Appendix C: Boson-fermion states

We calculate the negativities for maximally entangled states of a bosonic mode entangled with a fermionic one.

To start we consider the following states

$$|X_1\rangle = \frac{1}{\sqrt{2}} (|0_\omega\rangle_U |1_\Omega^F\rangle_U^+ + |1_\omega\rangle_U |1_\Omega^F\rangle_U^-), \quad (C1a)$$

$$|X_2\rangle = \frac{1}{\sqrt{2}} (|1_\omega\rangle_U^+ |1_\Omega^F\rangle_U^- + |1_\omega\rangle_U^- |1_\Omega^F\rangle_U^+), \quad (C1b)$$

where F labels the fermionic mode, ω, Ω are the frequencies and 0, 1 the occupation numbers of the Unruh-modes. + and - refer to particles and antiparticles, respectively. The mode of frequency ω is bosonic while the mode of frequency Ω is fermionic. The respective acceleration parameters are given by $r = \text{arctanh}(e^{-\frac{\pi\omega}{a_\omega}})$ for the bosonic and $r_f = \text{arctan}(e^{-\frac{\pi\Omega}{a_\Omega}})$ for the fermionic mode. The relevant part of the partially transposed reduced density matrices for these states can be computed to be

$$\frac{1}{2} \cos^2(r_f) \frac{\tanh^{2n}(r)}{\cosh^2(r)} \left(\frac{\frac{n}{\sinh^2(r)}}{\sqrt{\frac{n+1}{\cosh^2(r)}}} \sqrt{\frac{n+1}{\cosh^2(r)}} \tanh^2(r) \right) \quad (C2)$$

for state X_1 and

$$\frac{1}{2} \cos^2(r_f) \frac{\tanh^{2m+2n}(r)}{\cosh^6(r)} \times \left(\frac{n}{\sqrt{(m+1)(n+1)}} \sqrt{\frac{(m+1)(n+1)}{m}} \right) \quad (C3)$$

for state X_2 . We observe that the fermionic and the bosonic part factorize and so we find that the resulting negativity can be expressed in terms of negativities obtained from the cases of one accelerated observer. That

is

$$N_{X_1} = 2N_f N_{b,1}, \quad (C4)$$

$$N_{X_2} = 2N_f N_{b,2}, \quad (C5)$$

where N_f is the negativity $N_f = \frac{1}{2} \cos^2(r_f) = \frac{1}{2} (Z_F^\Omega)^{-1}$ and $N_{b,1}, N_{b,2}$ are given by

$$N_{b,1} = \frac{1}{2} \frac{1}{(Z_B^\omega)^2} + \sum_{n=1}^{\infty} N_n, \quad (C6)$$

$$N_{b,2} = \frac{1}{(Z_B^\omega)^3} \sum_{n,m=0}^{\infty} e^{-\frac{2\pi(n+m)}{a_\omega}} = \frac{1}{2} \frac{1}{Z_B^\omega}, \quad (C7)$$

i.e. the ones we obtain when we only accelerated the bosons. The N_n in (C6) can be obtained by setting $r^\Omega = 0$ in (B3) and are given by

$$N_n = \frac{\tanh^{2n}(r)}{2 \cosh^2(r)} \left(\frac{n}{2 \sinh^2(r)} + \frac{1}{2} \tanh^2(r) + \sqrt{\frac{n^2}{4 \sinh^4(r)} + \frac{\frac{n}{2} + \frac{1}{4} \sinh^2(r) \tanh^2(r) + 1}{\cosh^2(r)}} \right). \quad (C8)$$

Next we move to Bell states Ψ_{BF}^\pm and Φ_{BF}^\pm that are given by

$$|\Psi_{BF}^\pm\rangle = \frac{1}{\sqrt{2}} (|1_\omega\rangle_U |0_\Omega^F\rangle_U \pm |0_\omega\rangle_U |1_\Omega^F\rangle_U^\pm), \quad (C9a)$$

$$|\Phi_{BF}^\pm\rangle = \frac{1}{\sqrt{2}} (|0_\omega\rangle_U |0_\Omega^F\rangle_U \pm |1_\omega\rangle_U |1_\Omega^F\rangle_U^\pm). \quad (C9b)$$

The negativity of state Φ_{BF}^\pm is calculated in the following. After obtaining the reduced density matrix $\rho_{\Phi_{BF}^\pm}$ by tracing out region II

$$\begin{aligned} \rho_{\Phi_{BF}^\pm} = & \frac{\cos^2(r_f)}{2} \left\{ \sum_n \cos^2(r_f) a_n^2 |n\rangle\langle n| \otimes (|00\rangle\langle 00| + \tan^2(r_f) |10\rangle\langle 10|) + \sum_n \bar{a}_n^2 |(n+1)\rangle\langle (n+1)| \otimes |10\rangle\langle 10| \right. \\ & \left. + \sum_n \cos(r_f) a_n \bar{a}_n |n\rangle\langle (n+1)| \otimes |00\rangle\langle 10| + h.c. \text{nondiag.} \right\} \\ & + \frac{\sin^2(r_f)}{2} \left\{ \sum_n \cos^2(r_f) a_n^2 |n\rangle\langle n| \otimes (|01\rangle\langle 01| + \tan^2(r_f) |11\rangle\langle 11|) + \sum_n \bar{a}_n^2 |(n+1)\rangle\langle (n+1)| \otimes |11\rangle\langle 11| \right. \\ & \left. + \sum_n \cos(r_f) a_n \bar{a}_n |n\rangle\langle (n+1)| \otimes |01\rangle\langle 11| + h.c. \text{nondiag.} \right\}, \end{aligned} \quad (C10)$$

where $a_n = a_n(r) = \tanh^n(r) \cosh^{-1}(r)$, $\bar{a}_n = \bar{a}_n(r) = \tanh^n(r) \cosh^{-2}(r) \sqrt{n+1}$ and the notation $|ij\rangle = |i_\Omega\rangle_I^\dagger \otimes |j_\Omega\rangle_I^-$. Then after partial transposition, the relevant part of the reduced partially transposed density

matrix is of the form

$$\begin{pmatrix} 1 & 0 \\ 0 & \tan^2(r_f) \end{pmatrix} \otimes \rho^{pT}, \quad (C11)$$

where \otimes denotes the Kronecker product and

$$\rho^{pT} = \frac{1}{2} \cos^2(r_f) \frac{\tanh^{2n}(r)}{\cosh^2(r)} \times \begin{pmatrix} \cos^2(r_f) \frac{\tanh^2(r)}{\cosh^2(r)} & \cos(r_f) \sqrt{\frac{n+1}{\cosh^2(r)}} \\ \cos(r_f) \sqrt{\frac{n+1}{\cosh^2(r)}} & \frac{n}{\sinh^2(r)} + \sin^2(r_f) \end{pmatrix}. \quad (\text{C12})$$

Already at this stage we see that the fermionic contribution does not simply “factor out” as it was the case for states X_1 and X_2 . Due to the block diagonal form of (C11), the negativity $N_{\Phi_{BF}^\pm}$ can be written in the following form

$$N_{\Phi_{BF}^\pm} = \sum_n N_{\Phi_{BF}^\pm}^{(n)} = (1 + \tan^2(r_f)) \sum_n \tilde{N}_{\Phi_{BF}^\pm}^{(n)}, \quad (\text{C13})$$

where $\tilde{N}_{\Phi_{BF}^\pm}^{(n)}$ is the negativity calculated from (C12). Again one can see that each $N_{\Phi_{BF}^\pm}^{(n)}$ is bounded from above by $N_{\Phi_{BF}^\pm}^{(0)}$, see Figure 8c. To obtain $N_{\Phi_{BF}^\pm}^{(0)}$ we have to calculate $\tilde{N}_{\Phi_{BF}^\pm}^{(0)}$

$$\tilde{N}_{\Phi_{BF}^\pm}^{(0)} = 2N_f N_{0,\omega} e^{\frac{\Omega}{T_\Omega}} \left(\sqrt{n_F^\Omega n_B^\omega} - n_F^\Omega n_B^\omega \right), \quad (\text{C14})$$

where $n_B^\omega = (e^{\frac{\omega}{T_\omega}} - 1)^{-1}$ is the Bose-Einstein distribution, $N_{0,\omega}$ is given by (B6) and $n_F^\Omega = (e^{\frac{\Omega}{T_\Omega}} + 1)^{-1}$ is the Fermi-Dirac distribution and the $T_{\omega/\Omega}$ are the Unruh temperatures. Now we can use $N_{\Phi_{BF}^\pm}^{(0)} = (1 + \tan^2(r_f)) \tilde{N}_{\Phi_{BF}^\pm}^{(0)}$ to calculate

$$N_{\Phi_{BF}^\pm}^{(0)} = 2N_f N_{0,\omega} \gamma_{\Phi_{BF}^\pm}(n_B^\omega, n_F^\Omega), \quad (\text{C15})$$

where

$$\gamma_{\Phi_{BF}^\pm}(n_B^\omega, n_F^\Omega) = \sqrt{\frac{n_B^\omega}{n_F^\Omega}} - n_B^\omega. \quad (\text{C16})$$

The further $N_{\Phi_{BF}^\pm}^{(n)}$ for $n \neq 0$ can be obtained analytically and the negativity $N_{\Phi_{BF}^\pm}$ is obtained to be

$$N_{\Phi_{BF}^\pm} = N_{\Phi_{BF}^\pm}^{(0)} + \sum_{n=1}^{\infty} \frac{\tanh^{2n-2}(r)}{4 \cosh^4(r)} (n + \sinh^2(r) \cos^2(r_f) (\tanh^2(r) + \tan^2(r_f)) + \sqrt{n^2 + 2 \sinh^2(r) ((n+2) \tanh^2(r) \cos^2(r_f) + n \sin^2(r_f)) + \sinh^4(r) (\sin^2(r_f) - \tanh^2(r) \cos^2(r_f))^2}). \quad (\text{C17})$$

To obtain a condition for vanishing negativity, we have a look at (C16) and realize that the condition for entanglement can be written as

$$n_B^\omega n_F^\Omega \leq 1. \quad (\text{C18})$$

Finally, we calculate the negativity of state Ψ_{BF}^\pm . The relevant part of the reduced partially transposed density matrix is of the form

$$\begin{pmatrix} 1 & 0 \\ 0 & \tan^2(r_f) \end{pmatrix} \otimes \rho^{pT}, \quad (\text{C19})$$

where

$$\rho^{pT} = \frac{1}{2} \cos^2(r_f) \frac{\tanh^{2n}(r)}{\cosh^2(r)} \times \begin{pmatrix} \cos^2(r_f) \frac{n}{\sinh^2(r)} & \cos(r_f) \sqrt{\frac{n+1}{\cosh^2(r)}} \\ \cos(r_f) \sqrt{\frac{n+1}{\cosh^2(r)}} & \frac{n+1}{\cosh^2(r)} \sin^2(r_f) + \tanh^2(r) \end{pmatrix}. \quad (\text{C20})$$

Due to the structure of (C19) the negativity again has the form (C13). Then $N_{\Psi_{BF}^\pm}$ is calculated to be

$$\begin{aligned}
N_{\Psi_{BF}^{\pm}} = & N_{\Psi_{BF}^{\pm}}^{(0)} + \sum_{n=1}^{\infty} \frac{\tanh^{2n-2}(r)}{4 \cosh^4(r)} (\tanh^2(r) ((n+1) \sin^2(r_f) + \sinh^2(r)) + n \cos^2(r_f) + \\
& -2(\frac{n^2}{4} \cos^4(r_f) + \tanh^4(r)(\frac{n+1}{2} \sinh^2(r) \sin^2(r_f) + \frac{1}{4}(n+1)^2 \sin^4(r_f) + \frac{1}{4} \sinh^4(r)) + \\
& + \tanh^2(r) \cos^2(r_f)(\frac{n}{2} + 1) \sinh^2(r) - \frac{n+1}{2} n \sin^2(r_f)))^{\frac{1}{2}}, \tag{C21}
\end{aligned}$$

where

$$N_{\Psi_{BF}^{\pm}}^{(0)} = \frac{1}{2} \frac{1}{Z_F^{\Omega}} \frac{1}{(Z_B^{\omega})^2}. \tag{C22}$$

$N_{\Psi_{BF}^{\pm}}^{(0)}$ again gives an upper bound on all the $N_{\Psi_{BF}^{\pm}}^{(n)}$ and an lower bound on $N_{\Psi_{BF}^{\pm}}$, see Figure 8d.

Appendix D: Near horizon limit for a Schwarzschild black hole

In the presence of a Schwarzschild black hole the spacetime outside the black hole is characterized by the Schwarzschild metric

$$ds^2 = \left(1 - \frac{R_S}{r}\right) dt^2 - \frac{1}{1 - \frac{R_S}{r}} dr^2 - r^2 d\Omega^2, \tag{D1}$$

where G is the gravitational constant, M is the mass of the black hole, $R_S = 2GM$ is the Schwarzschild radius and $d\Omega^2$ is the line element of the unit 2-sphere. In order to obtain the limiting form of (D1) close to the horizon of a Schwarzschild black hole, we consider an observer placed at $r = r_0$ with proper time $\eta = (1 - 2GM/r_0)t$. Introducing

$$\rho^2 = 8GM(r - 2GM), \tag{D2}$$

we obtain the following metric up to terms of order $\frac{1}{2GM}$ in the near horizon limit

$$ds^2 = ds_R^2 - ds_2^2, \tag{D3}$$

where

$$ds_R^2 = \frac{1}{16G^2M^2} \left(1 - \frac{2GM}{r_0}\right)^{-1} \rho^2 d\eta^2 - d\rho^2, \tag{D4}$$

$$ds_2^2 = (2GM)^2 d\Omega^2. \tag{D5}$$

So (D1) reduces to the product of two-dimensional Rindler space (ds_R^2) and a 2-sphere of radius $2GM$ (ds_2^2). Comparing ds_R^2 to the two-dimensional Rindler metric (2) we see that the acceleration a experienced by an observer at fixed position $r = r_0$ is given by

$$a = \frac{1}{4GM} \left(1 - \frac{2GM}{r_0}\right)^{-\frac{1}{2}}. \tag{D6}$$

To extend the considerations of Sections III, IV and V in 2d Rindler space to this spacetime, we consider the wave equation for a massless scalar field ψ that is given by $\square\psi = 0$. In the near horizon limit (D3) we can write

$$(\square_R - \Delta_{S^2})\psi(\eta, \rho, \phi, \theta) = 0, \tag{D7}$$

where ϕ, θ are angular coordinates, \square_R is the d'Alembertian of 2d Rindler space and Δ_{S^2} is the Laplacian of the 2-sphere. We are looking for solutions of the form

$$\psi(\eta, \rho, \phi, \theta) = \psi_{rad}(\eta, \rho) \psi_{ang}(\phi, \theta), \tag{D8}$$

that satisfy

$$\square_R \psi_{rad}(\eta, \rho) = 0, \tag{D9}$$

$$\Delta_{S^2} \psi_{ang}(\phi, \theta) = 0. \tag{D10}$$

The solutions of (D9) are the well known solutions of the Klein Gordon equation in Rindler space that we used above. The eigenfunctions of Δ_{S^2} are given by the spherical harmonics $Y_l^m(\phi, \theta)$. The eigenvalues are $l(l+1)$. So we pick the eigenfunctions with $l = 0$, i.e.

$$\psi_{ang}(\phi, \theta) = e^{im\phi} P_{l=0}^m(\cos(\theta)) = 1, \tag{D11}$$

where the $P_l^m(\cos(\theta))$ are the associated Legendre polynomials. We conclude that for the choice $l = 0$, i.e. zero angular momentum, we can describe the near horizon limit by restricting our considerations to 2d Rindler space.

Therefore, in the following we restrict ourselves to wave functions ψ of vanishing angular momentum satisfying (D8). When we consider maximally entangled fermion states (16) to hover over a black hole at some distance $d = r_0 - R_S$ from the horizon, the system can be described in 2d Rindler space (for some more details on this correspondence see [19]). The analogue of the Rindler vacuum $|0\rangle_I$ is the Boulware vacuum $|0\rangle_B$ and the Unruh vacuum $|0\rangle_U$ corresponds to the Hartle-Hawking vacuum $|0\rangle_H$. Further, the physical effect that causes the degradation of entanglement is now the Hawking effect. Near to a black hole of mass M the acceleration a in (2) is set by (D6). So, we see that the limit of infinite acceleration corresponds to the limit of r_0 approaching R_S . Considering an observer stationary at a radial distance of r_0 , one

can write the acceleration parameter as

$$r = \text{arctanh}(e^{-\frac{\omega_g}{2} \sqrt{1 - \frac{R_S}{r_0}}}), \quad (\text{D12})$$

$$r_f = \text{arctan}(e^{-\frac{\omega_g}{2} \sqrt{1 - \frac{R_S}{r_0}}}), \quad (\text{D13})$$

where ω_g and Ω_g are the rescaled frequencies $\omega_g =$

$4\pi R_S \omega$ and $\Omega_g = 4\pi R_S \Omega$. Plugging the acceleration parameters (D12) and (D13) into the expressions for the negativities, we obtained above, one obtains the negativities of the respective states in the case that the acceleration is due to the presence of a black hole.

-
- [1] M. A. Nielsen and I. L. Chuang, *Quantum computation and quantum information* (Cambridge university press, 2010).
 - [2] S. L. Braunstein, S. Pirandola, and K. Życzkowski, Phys. Rev. Lett. **110**, 101301 (2013).
 - [3] A. Almheiri, D. Marolf, J. Polchinski, and J. Sully, J. High Energy Phys. **2013**, 1 (2013).
 - [4] I. Fuentes-Schuller and R. B. Mann, Phys. Rev. Lett. **95**, 120404 (2005).
 - [5] D. E. Bruschi, A. Dragan, A. R. Lee, I. Fuentes, and J. Louko, Phys. Rev. Lett. **111**, 090504 (2013).
 - [6] E. Martín-Martínez, D. Aasen, and A. Kempf, Phys. Rev. Lett. **110**, 160501 (2013).
 - [7] N. Friis, D. E. Bruschi, J. Louko, and I. Fuentes, Phys. Rev. D **85**, 081701 (2012).
 - [8] K. Brádler, P. Hayden, and P. Panangaden, J. High Energy Phys. **2009**, 074 (2009).
 - [9] N. Friis, A. R. Lee, K. Truong, C. Sabín, E. Solano, G. Johansson, and I. Fuentes, Phys. Rev. Lett. **110**, 113602 (2013).
 - [10] M. Montero and E. Martín-Martínez, J. High Energy Phys. **2011**, 1 (2011).
 - [11] P. M. Alsing, I. Fuentes-Schuller, R. B. Mann, and T. E. Tessier, Phys. Rev. A **74**, 032326 (2006).
 - [12] Q. Pan and J. Jing, Phys. Rev. A **77**, 024302 (2008).
 - [13] E. Martín-Martínez and J. León, Phys. Rev. A **80**, 042318 (2009).
 - [14] D. E. Bruschi, J. Louko, E. Martín-Martínez, A. Dragan, and I. Fuentes, Phys. Rev. A **82**, 042332 (2010).
 - [15] E. Martín-Martínez and I. Fuentes, Phys. Rev. A **83**, 052306 (2011).
 - [16] Q. Pan and J. Jing, Phys. Rev. D **78**, 065015 (2008).
 - [17] E. Martín-Martínez and J. León, Phys. Rev. A **81**, 032320 (2010).
 - [18] D. E. Bruschi, A. Dragan, I. Fuentes, and J. Louko, Phys. Rev. D **86**, 025026 (2012).
 - [19] E. Martín-Martínez, L. J. Garay, and J. León, Phys. Rev. D **82**, 064006 (2010).
 - [20] J. León and E. Martín-Martínez, Phys. Rev. A **80**, 012314 (2009).
 - [21] M. Montero and E. Martín-Martínez, Phys. Rev. A **84**, 012337 (2011).
 - [22] E. Martín-Martínez and J. León, Phys. Rev. A **81**, 052305 (2010).
 - [23] J. Chang and Y. Kwon, Phys. Rev. A **85**, 032302 (2012).
 - [24] M. Shamirzaie, B. N. Esfahani, and M. Soltani, Int. J. Theor. Phys. **51**, 787 (2012).
 - [25] S. Khan, N. A. Khan, and M. Khan, Commun. Theor. Phys. **61**, 281 (2014).
 - [26] J. Wang and J. Jing, Phys. Rev. A **83**, 022314 (2011).
 - [27] D. Ahn and M. Kim, Phys. Rev. A **366**, 202 (2007).
 - [28] G. Adesso, I. Fuentes-Schuller, and M. Ericsson, Phys. Rev. A **76**, 062112 (2007).
 - [29] A. Dragan, J. Doukas, E. Martín-Martínez, and D. E. Bruschi, Class. Quant. Grav. **30**, 235006 (2013).
 - [30] A. Dragan, J. Doukas, and E. Martín-Martínez, Phys. Rev. A **87**, 052326 (2013).
 - [31] J. Doukas, E. G. Brown, A. Dragan, and R. B. Mann, Phys. Rev. A **87**, 012306 (2013).
 - [32] G. Adesso, S. Ragy, and D. Girolami, Class. Quant. Grav. **29**, 224002 (2012).
 - [33] N. D. Birrell and P. C. W. Davies, *Quantum fields in curved space*, 7 (Cambridge university press, 1984).
 - [34] S. Takagi, Prog. Theor. Phys. Suppl. **88**, 1 (1986).
 - [35] W. G. Unruh, Phys. Rev. D **14**, 870 (1976).
 - [36] G. Vidal and R. F. Werner, Phys. Rev. A **65**, 032314 (2002).
 - [37] A. Peres, Phys. Rev. Lett. **77**, 1413 (1996).
 - [38] M. Horodecki, P. Horodecki, and R. Horodecki, Phys. Lett. A **223**, 1 (1996).
 - [39] N. Friis, A. R. Lee, and D. E. Bruschi, Phys. Rev. A **87**, 022338 (2013).
 - [40] M. Horodecki, P. Horodecki, and R. Horodecki, Phys. Rev. Lett. **80**, 5239 (1998).
 - [41] M. Montero, J. León, and E. Martín-Martínez, Phys. Rev. A **84**, 042320 (2011).
 - [42] R. Simon, Phys. Rev. Lett. **84**, 2726 (2000).
 - [43] S. W. Hawking, Commun. Math. Phys. **43**, 199 (1975).
 - [44] S. W. Hawking, Phys. Rev. D **14**, 2460 (1976).